

Detectors Techniques for Cosmology and Astroparticle Physics Poster Session Review

Conveners:

Luciano Gottardi (SRON - Netherlands Institute for Space Research)

Regina Caputo (NASA Goddard Space Flight Center)

Topics Covered

- ▶ Dark matter, Rare Events, and New Physics
- ▶ Neutrino Astronomy and Physics
- ▶ Gravitational Wave and Multimessenger Astrophysics
- ▶ X-ray and Gamma-ray Telescopes
- ▶ Cosmic rays and Antimatter
- ▶ Other Astrophysics Detectors

Dark Matter, Rare Events & New Physics

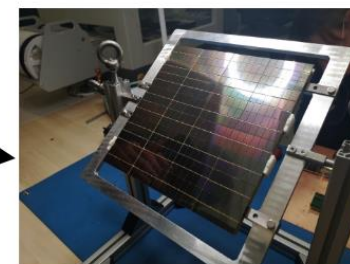
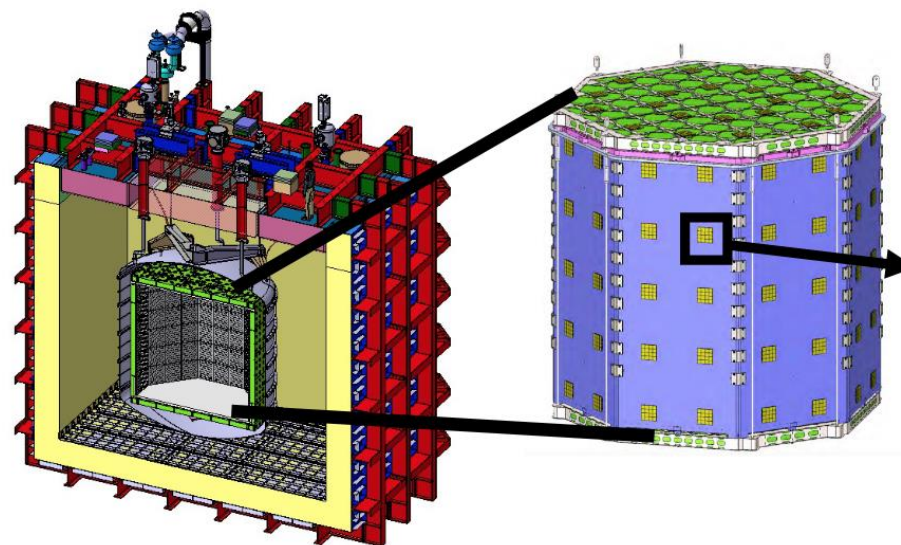
WIMPs, Dark Photons, Neutrino-less double beta decay, Sterile Neutrinos
Nobel liquids, solid state devices, calorimeters

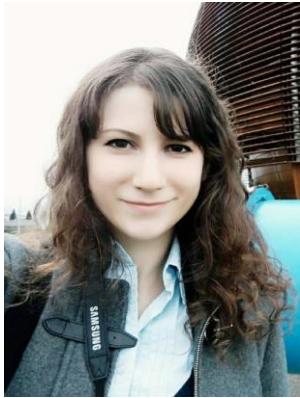


The Darkside-20k neutron veto and its light detectors

Daria Santone, RHUL
On behalf of Darkside-20k
collaboration

Darkside-20k is a global direct dark matter search experiment situated at Laboratori Nazionali del Gran Sasso, **designed to reach a total exposure of 200 tonne-years free from instrumental background**. The most dangerous background to the dark matter search comes from nuclear recoils induced by radiogenic neutrons, since this process can mimic a dark matter scattering-induced recoil. The DarkSide-20k detector has a novel design in which the neutron veto and the TPC are integrated into a single mechanical unit that sits in a common bath of low-radioactivity argon. The entire TPC wall is surrounded by a Gd-PMMA shell which is equipped with large area Silicon Photomultiplier (SIPMs) array detectors. SiPMs are disposed in a compact design designed to minimise the number of Printed Circuit Boards (PCBs), cables and connectors, called photodetection unit (vPDU). The preliminary results of first vPDU+ and the expected neutron veto performances will be discussed.





Valentina Cicero

An imaging detector for liquid scintillator experiments

Valentina Cicero
on behalf of the PRIN 2017KC8WMB group
PM2021 - 15th Pisa Meeting on Advanced Detectors

INTRODUCTION

Noble elements in the liquid phase (LAr, LXe) constitute an excellent medium for the detection of Neutrino interactions and for Dark Matter searches. We are developing an optical system that collects the **scintillation light** produced by charged particles in this medium to perform a **fast 3D reconstruction** of events, as an alternative or complement to Time Projection Chambers.

The base unit system consists in a "Camera" composed by a **Coded Aperture Mask** and a **Silicon Photomultiplier (SiPM)** matrix.

Properties:

- High rate capability
- Feasibility to work in a magnetic field
- SiPM VUV models can detect scintillation LAr scintillation light (PDE ~15 % @ 128 nm)
- High noise reduction at low temperature
- Coded mask have ~50% photon transmission by construction
- Deep and wide field of view

CODED APERTURE MASKS

Coded aperture mask techniques were developed as the evolution of a single pinhole camera.

A matrix of multiple pinholes improves light collection and reduces exposure time.

The image formed on the sensor is the superposition of multiple pinhole images.

The original image is obtained with a simple deconvolution process where the kernel is derived from the mask pattern.

The detailed technique and preliminary results with simulated neutrino events are described in: M. Andreani et al., "Tolled masks for imaging of neutrino events", European Physical Journal C, 2021, 81:1011

EXAMPLE DETECTOR GEOMETRY

Neutrino events have been simulated in an example detector geometry of ~1 ton LAr target volume.

• 150 x 140 x 60 cm³

• 76 cameras, covering most of the available surface

• 32x32 matrix sensors, 3x3 mm² pixels

• Full SiPM waveform simulation and readout electronics included in event reconstruction

3D DIRECT RECONSTRUCTION ALGORITHM

- Each hit on the SiPM matrix is propagated back into the inner volume through every hole in the mask, with an appropriate **weight** assigned to voxels.
- This weight represents the **Bayesian probability** of the voxel to be a source of the detected photons.
- A score in the segmented reconstruction volume is calculated by adding these weights.

Software written in Python and openCL for GPU acceleration.

Compared to traditional techniques, this algorithm is well suited to deal with low light yields.

NEUTRINO EVENTS RECONSTRUCTION

The algorithm reconstructs a map of the deposited energy in the volume, where a higher voxel score corresponds to a higher probability of being the source of the scintillation photons.

Challenges:

- Cameras crossed by particles loose information → ML algorithms under development to detect and exclude these cameras.
- Low contrast between signal and background voxels: voxel selection cut is not trivial.
- Track points extraction with local principal curvatures algorithm.

PROTOTYPE

We're building a prototype demonstrator with 3 cameras based on available SiPM matrices on the market, with cryogenic electronics.

Each camera consists in:

- 4 Hamamatsu S14161 8x8 matrices, with 3x3 mm² SiPM, coated in TPB wavelength shifter.
- 8 ALICORs, a 32-channel cryogenic ASIC with multiple TDCs, developed by INFN Torino microelectronics group

Camera placement scheme inside cryostat.

SiPM matrix board

ALICOR

This prototype will be tested in a Liquid Argon cryostat for imaging of simple light sources and cosmic rays, at ARTIC facility in INFN Genova. Expected Q2 2023.

An Imaging detector for noble liquid experiments

V. Cicero on behalf of the PRIN 2017KC8WMB group

- We are developing an optical system that collects the **scintillation light** produced by charged particles in **noble liquid elements** (LAr, LXe) to perform a **fast 3D reconstruction** of events, as an alternative or complement to Time Projection Chambers.
- The basic unit of this system is a camera that consists in a **coded aperture mask** and a Silicon Photomultiplier (SiPM) matrix.
- We developed a **3D reconstruction algorithm** based on a weighted back-propagation approach that reconstructs a map of the deposited energy in the volume. This algorithm improves on the performances of traditional techniques when a low number of photons is detected.
- Full simulation and reconstruction of neutrino events have been performed in a ~1 ton LAr cryostat geometry, equipped with 76 coded aperture mask cameras.
- We are building a **prototype** with 3 cameras based on available SiPM matrices on the market, and with cryogenics electronics. First tests in Liquid Argon are expected in Q2 2023.



Giorgio Dho



Part of this project has been funded by the European Union's Horizon 2020 research and innovation programme under the ERC Consolidator Grant Agreement No. 818744.

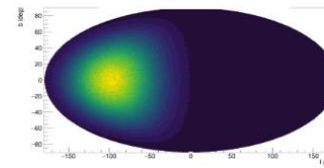


THE CYGNO EXPERIMENT, A DIRECTIONAL DETECTOR FOR DIRECT DARK MATTER SEARCHES

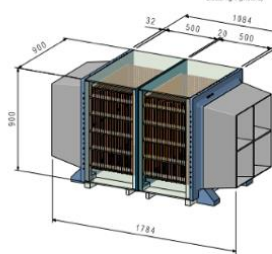
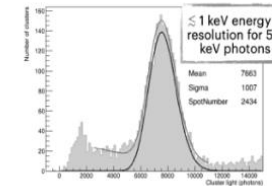


G. Dho on behalf of CYGNO coll.
Gran Sasso Science Institute, L'Aquila, Italy

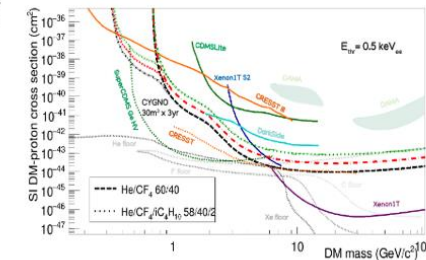
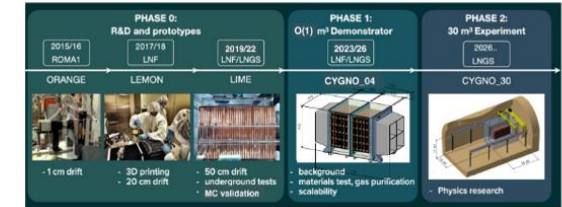
- Detector for diirectional Dark Matter searches
- CYGNO future phases to be hosted at LNGS
- Recent result promising for the detector operation
- CYGNO_04 already under design
- CYGNO_30 expected physics performances under evaluation together with R&D development



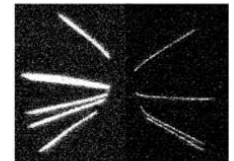
Simulation of F recoils in Galactic coord



Detector Vol = 0.66x0.66x1.03 = 0.4 Mc



PRELIMINARY





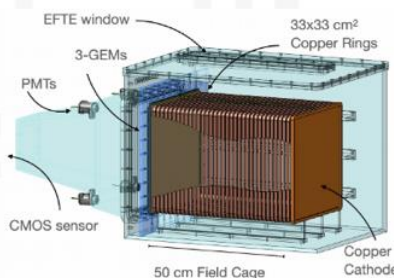
Flaminia Di Giambattista

LIME: a gas TPC prototype for directional Dark Matter search for the CYGNO experiment

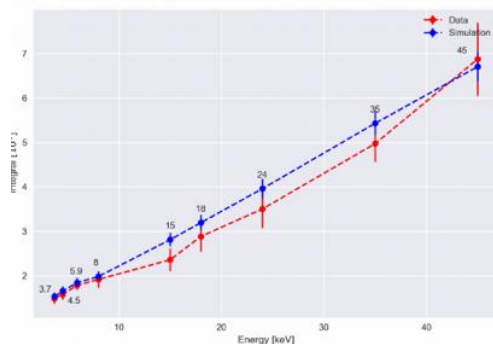
F. Di Giambattista^{1,2} on behalf of the CYGNO Collaboration

¹Gran Sasso Science Institute, 67100 L'Aquila, Italy

²INFN, Laboratori Nazionali del Gran Sasso, 67100 Assergi, Italy

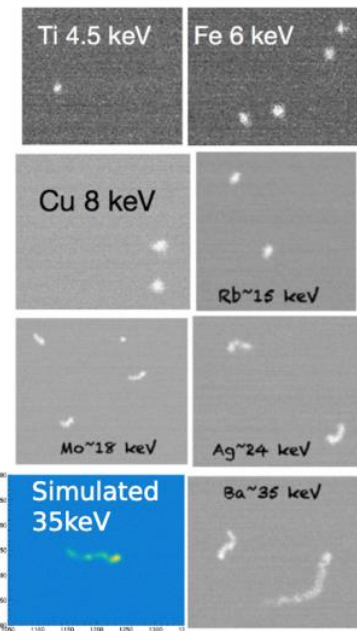


- Looking for DM through directional signature of low energy nuclear recoils (NR)
- LIME 50L prototype, now installed underground at LNGS
 - Gaseous TPC with GEM charge amplification and optical readout (1 sCMOS camera + 4 PMTs)
- Tested overground at LNF with radioactive X-ray sources



- Measured energy resolution of $\sim 15\%$ at 6 keV (^{55}Fe)
- Stability tested for 1 month
- Response is linear and consistent with Monte Carlo (MC) simulation
- MC simulation of sCMOS images to study track shape and detector's response

- MC simulation of background at LNGS (in view of the upcoming data taking campaign - background characterization, MC validation, neutron flux spectral measurement)



15th Pisa Meeting on Advanced Detectors - La Biodola, Isola d'Elba, May 22-28, 2022

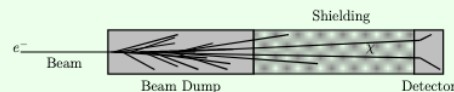
The BDX-MINI detector for Light Dark Matter search @ JLAB

Spreafico M. on behalf of BDX Collaboration
marco.spreafico@ge.infn.it



Light Dark Matter

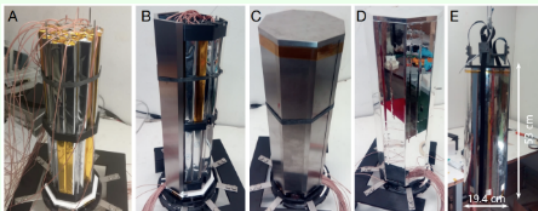
- Light Dark Matter (LDM) is a new compelling hypothesis that identifies Dark Matter with new sub-GeV states interacting with ordinary matter through a new force. This interaction can be mediated by a massive vector boson called "Dark Photon".
- In beam dump experiments, a high intensity beam impinges on a thick material (beam dump), producing a forward focused secondary LDM beam
- A sizable shielding located downstream the dump absorbs all SM particles except neutrinos
- LDM particles are detected through their scattering in a downstream detector. BDX-MINI aims at detecting $\chi - e$ elastic scattering in an electromagnetic calorimeter



BDX-MINI Detector

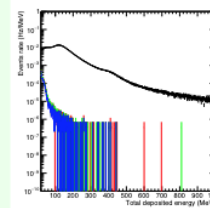
BDX-MINI detector is composed of an ECal surrounded by a multi layer veto:

- ECal is made up of 44 PbWO₄ crystals for a total active volume of 4 dm³ (A)
 - 32 (15 × 15 × 200 mm³) spare CLAS-12 FT crystals glued in pairs
 - 28 (20 × 20 × 200 mm³) spare PANDA ECal crystals
 - Readout: 6 × 6 mm² Hamamatsu MPPCs (S13360-6025PE)
 - LY: 1 p.e. / MeV
- The veto is composed of three layers:
 - Innermost layer: passive tungsten shielding 0.8 cm thick (B, C)
 - Middle (D) and Outer (E) layer made by 0.8 cm thick plastic scintillator read with WLS fibers and 3×3 Hamamatsu S13360-3075CS SiPMs
 - Octagonal Inner Veto composed by 8 paddles coupled with optical glue
 - Cylindrical Outer Veto composed by a single cylindrical tube
 - Number of readout channels for each active veto: 10 (8 for lateral, 2 for bases)
- Data acquisition:
 - Bias voltage provided by a custom designed board
 - SiPMs connected to front-end electronics via 8 m long coaxial cable (low noise)
 - Custom transimpedance amplifier with different gains for ECal and Veto channels
 - CAEN FPGA v1495 used for custom trigger logic
 - Digitalization with CAEN (v1730 and v1725) Flash ADC converter



Veto Performance

- High rejection capability combining the information from the two veto systems: at the MIP peak, counting rate suppressed of a factor 3800
- Veto rejection efficiency is similar for both vetoes independently of the veto shape
- Redundant readout compensates the potential inefficiency of the single SiPM
- The anti-coincidence requirement has a negligible effect on the signal detection efficiency



BDX-MINI Experiment

BDX-MINI experiment is a Beam Dump eXperiment running at Jefferson Lab. It aims to search for DM produced by the CEBAF high intensity e^- -beam impinging on the experimental Hall-A beam dump:

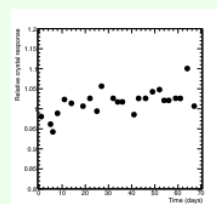
- e^- beam with $E_{\text{beam}} = 2.176$ GeV, current up to 150 μA
- Hall-A beam dump: 3 m Al + water cooling system
- detector positioned in a well 26 m downstream of the dump at beamline height
- Entire experimental setup situated within a sturdy field tent

BDX-MINI ran for 6 months in spring-summer 2020, collecting about 2.56×10^{21} EOT.



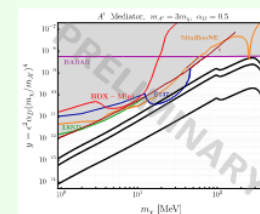
ECal Performance

- ECal calibration with special 10 GeV run
- Stability checked using cosmic muons
- Detector stable within $\sim 10\%$



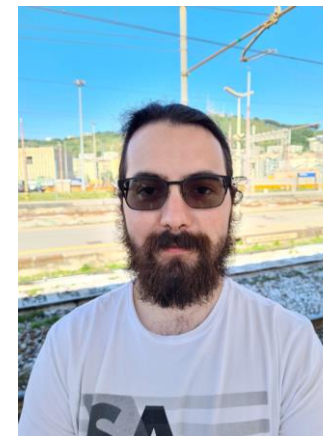
Physics Results

Evaluation of exclusion limit (90% C.L.) in the LDM parameter space



References

- Battaglieri M. et al arXiv:1707.04591
- Battaglieri M. et al. Eur. Phys. J. C (2021) 81: 164



Marco Spreafico



Laura Manenti

SEARCHING FOR DARK PHOTONS USING
A MULTILAYER DIELECTRIC HALOSCOPE

Dr. Laura Manenti

جامعة نيويورك أبوظبي
NYU ABU DHABI

THE DARK PHOTON

Dark photon is a hypothetical particle, a cousin of the photon, but it does not interact with ordinary matter. It is a massless particle, which means it travels at the speed of light. It is a vector boson, which means it has spin 1. It is a gauge boson, which means it is associated with a gauge symmetry. It is a dark gauge boson, which means it is associated with a dark gauge symmetry. It is a dark photon, which means it is a photon in the dark sector. It is a dark photon, which means it is a photon in the dark sector. It is a dark photon, which means it is a photon in the dark sector.

DIELECTRIC HALOSCOPE

A dielectric haloscope is a device used to search for dark photons. It consists of a stack of alternating dielectric layers, a lens, and a photosensor. The stack of dielectric layers is used to convert dark photons into ordinary photons. The lens is used to focus the ordinary photons onto the photosensor. The photosensor is used to detect the ordinary photons. The dielectric haloscope is a sensitive device for searching for dark photons. It is a sensitive device for searching for dark photons. It is a sensitive device for searching for dark photons.

MuDH (Multilayer Dielectric Haloscope Investigation)

The MuDH experiment is a search for dark photons using a dielectric haloscope. It consists of a stack of alternating dielectric layers, a lens, and a photosensor. The stack of dielectric layers is used to convert dark photons into ordinary photons. The lens is used to focus the ordinary photons onto the photosensor. The photosensor is used to detect the ordinary photons. The MuDH experiment is a sensitive device for searching for dark photons. It is a sensitive device for searching for dark photons. It is a sensitive device for searching for dark photons.

OBSERVED UPPER LIMITS

The MuDH experiment has observed upper limits on the dark photon-photon coupling constant. The upper limits are shown in the plot. The upper limits are shown in the plot. The upper limits are shown in the plot. The upper limits are shown in the plot. The upper limits are shown in the plot. The upper limits are shown in the plot. The upper limits are shown in the plot. The upper limits are shown in the plot. The upper limits are shown in the plot. The upper limits are shown in the plot.

CONCLUSION

The MuDH experiment has observed upper limits on the dark photon-photon coupling constant. The upper limits are shown in the plot. The upper limits are shown in the plot. The upper limits are shown in the plot. The upper limits are shown in the plot. The upper limits are shown in the plot. The upper limits are shown in the plot. The upper limits are shown in the plot. The upper limits are shown in the plot. The upper limits are shown in the plot. The upper limits are shown in the plot.

85% IS DARK MATTER

WITH WIMPS BECOMING LESS MOTIVATED,
ALTERNATIVE MODELS ARE GAINING TRACTION

THE DARK PHOTON IS
ONE OF THEM

1.5 eV

WE SEARCH FOR DP
WITH A MASS
AROUND 1.5 eV
USING A DIELECTRIC
HALOSCOPE

THE EXPERIMENT IS CALLED MUDHI, WHICH IN
ARABIC MEANS "LUMINOUS." IT'S THE FIRST
DM EXPERIMENT EVER BEEN OPERATED IN THE
MIDDLE EAST!

A DIELECTRIC HALOSCOPE IS
COMPOSED OF THREE PART:
A STACK OF TWO
ALTERNATING DIELECTRICS,
A LENS, A PHOTENSOR.

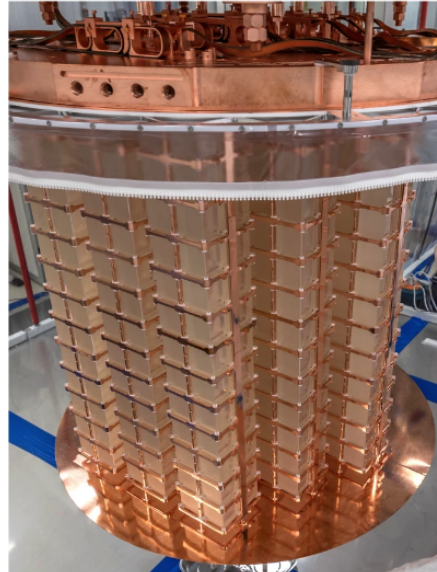
THE STACK COVERTS DARK
PHOTONS INTO ORDINARY
PHOTONS, WHICH GET
FOCUSSED AND DETECTED BY
THE PHOTENSOR.

WE DO NOT SEE AN EXCESS
OF SIGNAL EVENTS ABOVE
OUR BACKGROUND, SO WE
PLACE UPPER LIMITS ON
THE DARK PHOTON-PHOTON
COUPLING CONSTANT AT
90% C.L.



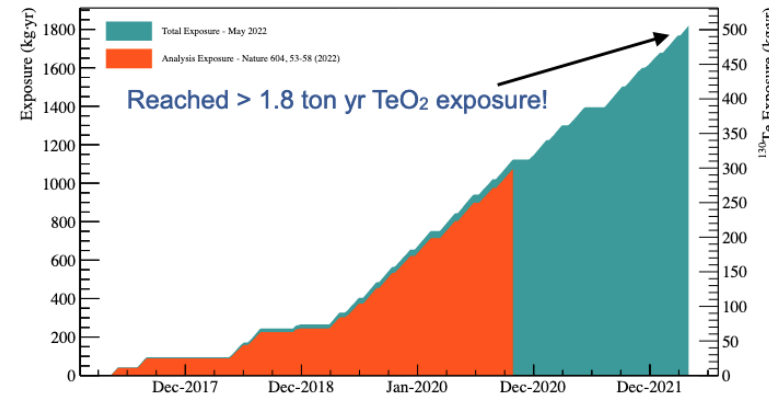
Latest results from the CUORE experiment

Irene Nutini (on behalf of the CUORE collaboration)
Università degli Studi Milano Bicocca - INFN Milano Bicocca



CUORE (Cryogenic Underground Observatory for Rare Events)

TeO₂ crystals: $\beta\beta$ source material, operated as cryogenic calorimeters



- In operation since 2017: optimisation campaigns
- Physics data taking at 11-15 mK since 2019. Data taking rate ~50 kg/month. Uptime ~90%

Data analysis

- Optimal Trigger: lower energy thresholds (< 10 keV)
- Denoising of the continuous data, using accelerometers & microphones

Physics results

- Search for ^{130}Te $0\nu\beta\beta$ decay: $T_{0\nu}^{1/2} (^{130}\text{Te}) > 2.2 \times 10^{25} \text{ yr}$ [$\sim 1 \text{ ton yr TeO}_2 \text{ exposure}$]
- Measurement of ^{130}Te $2\nu\beta\beta$ decay: $T_{2\nu}^{1/2} (^{130}\text{Te}) = [7.71^{+0.08}_{-0.06}(\text{stat})^{+0.12}_{-0.15}(\text{syst})] \times 10^{20} \text{ yr}$
- ^{130}Te $\beta\beta$ decay to excited states: $(T^{1/2})^{0\nu_{0+}} > 5.9 \times 10^{24} \text{ yr}$, $(T^{1/2})^{2\nu_{0+}} > 1.3 \times 10^{24} \text{ yr}$
- ^{120}Te $0\nu\beta+EC$ decay: $T_{0\nu}^{1/2} (^{120}\text{Te}) > 2.9 \times 10^{22} \text{ yr}$
- ^{128}Te $0\nu\beta\beta$ decay: $T_{0\nu}^{1/2} (^{128}\text{Te}) > 3.6 \times 10^{24} \text{ yr}$
- Other analysis: thermal model, background model and spectral shape studies, dark matter at low energy, high multiplicity events, ...



The LEGEND-200 LAr instrumentation in the search of neutrinoless double beta decay

Nina Burlac on behalf of LEGEND Collaboration

LEGEND-200 overview

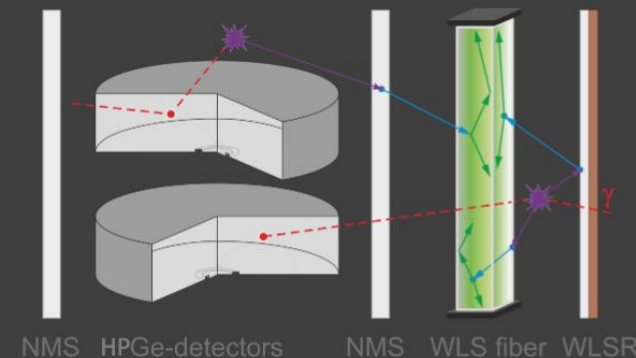
590 m³ tank with
ultra-pure water

WLSR
cylinder

64 m³ LAr
cryostat

WLS fiber curtains +
HPGe detector
array inside NMS

LAr instrumentation



- Detection of Ar scintillation light created by energy depositions in the LAr that accompanies energy depositions in the HPGe detectors;
- such background events originate from α , β , γ or neutron interactions, originating from primordial, anthropogenic radioisotopes or cosmogenic produced unstable isotopes;
- they must be discriminated from $0\nu\beta\beta$ decay signals, which have energy deposition inside the HPGe detectors and no energy deposition in the LAr.

Acronyms

HPGe – high-purity germanium	SIPM – silicon photomultiplier
LAr – liquid argon	WLS – wavelength shifting
NMS – nylon mini-shrouds	WLSR – WLS reflector



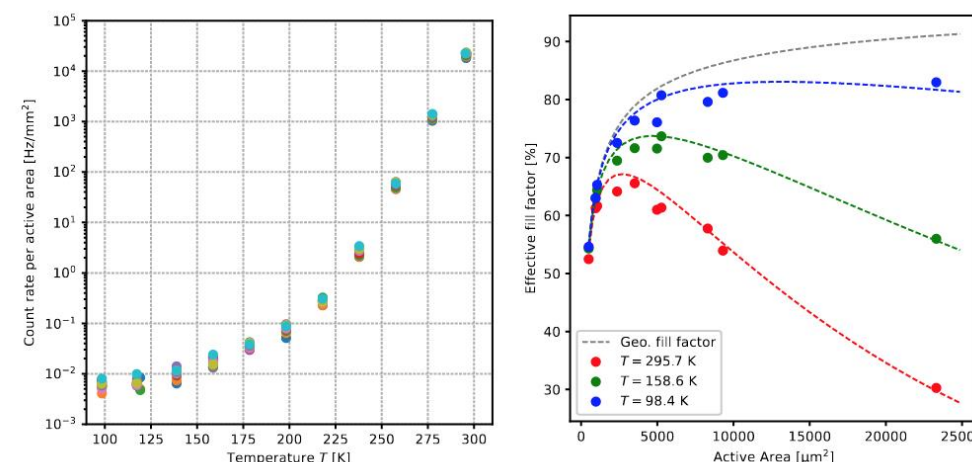
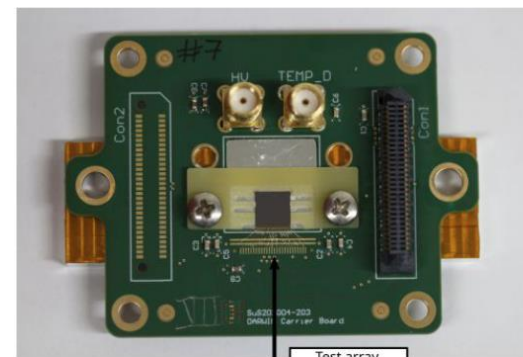


Michael Keller

SPAD Array Chips with Integrated Readout with High Fill Factor and Low Dark Count Rate at Low Temperatures

- We tested the suitability of Digital SiPMs as light detector for rare event search experiments using Liquid noble gases. Here, low dark count rate and a good photon sensitivity are required.
- A test array was developed with focus on a high fill factor and a low dark count rate. The latter was optimized by modifying the SPAD electric field.
- At liquid Xenon Temperatures ($T = 165\text{K}$) a dark count rate of 0.02 Hz/mm^2 (active area) was observed.
- The defect density on the wafer was determined, and with that a SPAD size found for which the fill factor is highest after switching off the defect affected/noisy SPADs.
- Based on these results a high fill factor array with a realistic, low power readout architecture for rare event searches was implemented.

Michael Keller, Peter Fischer, Heidelberg University





Massimiliano Nastasio

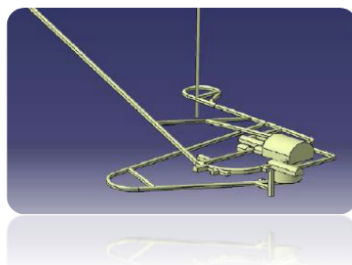


Novel High Sensitivity Analysis for Determination of Ultra-Trace Elements in Liquid Samples



G. Baccolo ^[1], A. Barresi ^[1], D. Chiesa ^[1], D. Merli ^[2], M. Nastasi ^{*(1)}, E. Previtali ^[1], M. Sisti ^[1]

University and INFN of Milano-Bicocca, Milano (Italy) ^[1] - University of Pavia, Pavia (Italy) ^[2]



In **rare event experiments** **sensitivity** is conditioned by the **radioactive background** present in the materials of the experimental apparatus



An **essential condition** to reduce background is to develop high-sensitivity analysis techniques in order to **select the most suitable materials**



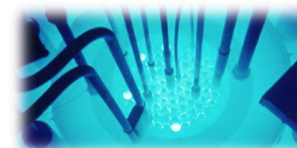
Radiopurity acceptable levels for ^{238}U and ^{232}Th : $1 \cdot 10^{-13}$ - $1 \cdot 10^{-15}$ g/g

High sensitivity analysis for the determination of ^{238}U and ^{232}Th in organic liquids

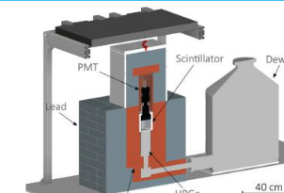
Radiochemical Treatments



Neutron Activation Analysis



β - γ measurements



Sensitivity achieved:
 $2 \cdot 10^{-15}$ g/g for ^{238}U - $1,5 \cdot 10^{-14}$ g/g for ^{232}Th



Frontier Detectors for Frontier Physics - 15th Pisa Meeting on Advanced Detectors
La Biodola, Isola d'Elba, May 22-28, 2022

*Corresponding Author.
E-mail address: massimiliano.nastasi@unimib.it

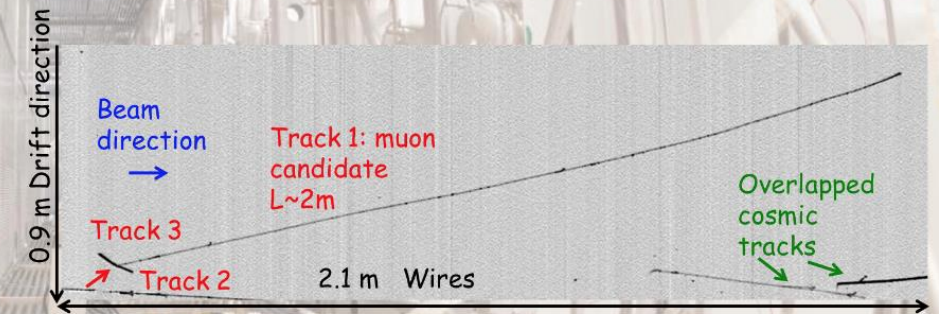


Laura Pasqualini

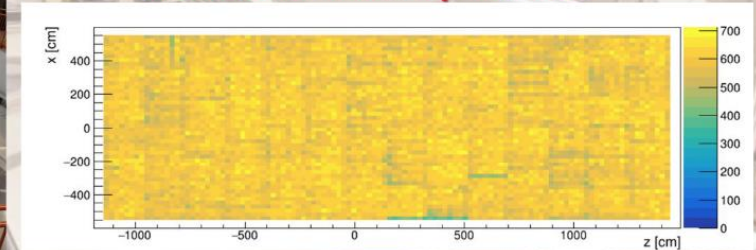
Short-Baseline neutrino oscillation searches with the ICARUS detector at FNAL

- The Short-Baseline Neutrino (SBN) program aims to confirm or definitely rule out the existence of sterile neutrinos at the eV mass scale by measuring the ν_e appearance and the ν_μ disappearance oscillation channel by means of Liquid Argon Time Projection Chambers (LArTPC) at Near (110 m) and Far (600 m) positions along the Booster neutrino beam at Fermilab.
- The SBN Far Detector, ICARUS T600, is a self-triggering detector with 3D imaging and calorimetric capabilities allowing accurate reconstruction of neutrino interactions.
- A Cosmic Ray Tagger (CRT) system ensuring a 4π coverage of ICARUS T600 is used to distinguish cosmics entering the detector from particles originated inside the TPC.

L. Pasqualini (INFN and University of Bologna)



Reconstructed hit positions



Calibration of the ICARUS cryogenic photo-detection system at FNAL

M. Bonesini¹, R. Benocci¹, R. Bertoni¹, A. Chatterjee², M. Diwan³, A. Menegolli⁴, G. Raselli⁴, M. Rossella⁴, A. Scarpelli³, N. Suarez²
for the ICARUS Collaboration

¹University and INFN Sezione di Milano Bicocca (Italy); ²University of Pittsburg (USA); ³BNL (USA); ⁴University and INFN Sezione di Pavia (Italy)

Calibration of the ICARUS cryogenic photo-detection system at FNAL

M. Bonesini¹, R. Benocci¹, R. Bertoni¹, A. Chatterjee², M. Diwan³, A. Menegolli⁴, G. Raselli⁴, M. Rossella⁴, A. Scarpelli³, N. Suarez²
for the ICARUS Collaboration

¹University and INFN Sezione di Milano Bicocca (Italy); ²University of Pittsburg (USA); ³BNL (USA); ⁴University and INFN Sezione di Pavia (Italy)

Calibration of the ICARUS cryogenic photo-detection system at FNAL

M. Bonesini¹, R. Benocci¹, R. Bertoni¹, A. Chatterjee², M. Diwan³, A. Menegolli⁴, G. Raselli⁴, M. Rossella⁴, A. Scarpelli³, N. Suarez²
for the ICARUS Collaboration

¹University and INFN Sezione di Milano Bicocca (Italy); ²University of Pittsburg (USA); ³BNL (USA); ⁴University and INFN Sezione di Pavia (Italy)

Calibration of the ICARUS cryogenic photo-detection system at FNAL

M. Bonesini¹, R. Benocci¹, R. Bertoni¹, A. Chatterjee², M. Diwan³, A. Menegolli⁴, G. Raselli⁴, M. Rossella⁴, A. Scarpelli³, N. Suarez²
for the ICARUS Collaboration

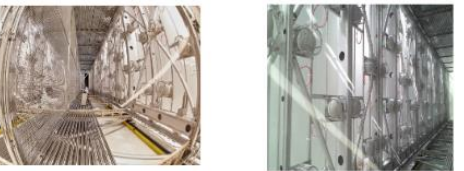
¹University and INFN Sezione di Milano Bicocca (Italy); ²University of Pittsburg (USA); ³BNL (USA); ⁴University and INFN Sezione di Pavia (Italy)

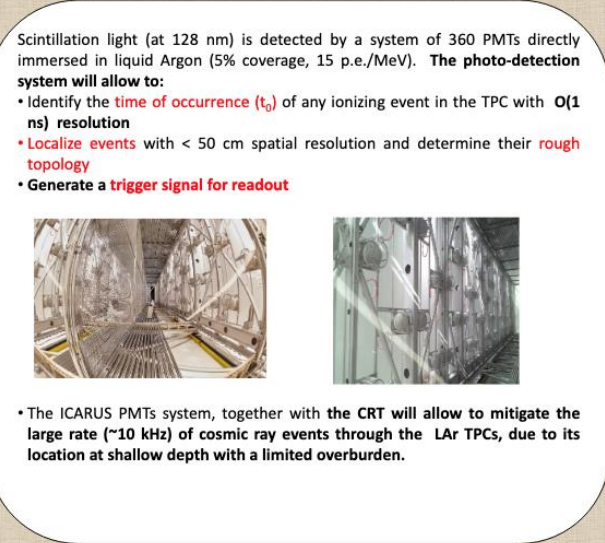
Scintillation light (at 128 nm) is detected by a system of 360 PMTs directly immersed in liquid Argon (5% coverage, 15 p.e./MeV). **The photo-detection system will allow to:**

- Identify the **time of occurrence (t_0)** of any ionizing event in the TPC with **0(1 ns) resolution**
- **Localize events** with < 50 cm spatial resolution and determine their **rough topology**
- **Generate a trigger signal for readout**

The image consists of two side-by-side photographs. The left photograph shows the interior of a large, cylindrical detector vessel, which is the ICARUS detector. The structure is complex, with many support beams and cables visible. A person is standing in the center of the vessel to provide a sense of scale. The right photograph is a close-up view of the PMT array, showing a dense arrangement of photomultiplier tubes mounted on a metal frame.

• The ICARUS PMTs system, together with the **CRT will allow to mitigate the large rate (~10 kHz) of cosmic ray events** through the **LAr TPCs**, due to its location at shallow depth with a limited overburden.

- Scintillation light (at 128 nm) is detected by a system of 360 PMTs directly immersed in liquid Argon (5% coverage, 15 p.e./MeV). **The photo-detection system will allow to:**
- Identify the **time of occurrence (t_0)** of any ionizing event in the TPC with **0(1 ns) resolution**
 - **Localize events** with < 50 cm spatial resolution and determine their **rough topology**
 - **Generate a trigger signal for readout**
- 
- The ICARUS PMTs system, together with the **CRT will allow to mitigate the large rate (~10 kHz) of cosmic ray events** through the LAr TPCs, due to its location at shallow depth with a limited overburden.



Scintillation light (at 128 nm) is detected by a system of 360 PMTs directly immersed in liquid Argon (5% coverage, 15 p.e./MeV). **The photo-detection system will allow to:**

- Identify the **time of occurrence (t_0)** of any ionizing event in the TPC with **0(1 ns) resolution**
- **Localize events** with < 50 cm spatial resolution and determine their **rough topology**
- **Generate a trigger signal for readout**

The image consists of two side-by-side photographs. The left photograph shows the interior of a large, cylindrical detector vessel, which is the ICARUS detector. The structure is complex, with many support beams and cables visible. A person is standing in the center of the vessel to provide a sense of scale. The right photograph is a close-up view of the PMT array, showing a dense arrangement of photomultiplier tubes mounted on a metal frame.

• The ICARUS PMTs system, together with the **CRT will allow to mitigate the large rate (~10 kHz) of cosmic ray events** through the **LAr TPCs**, due to its location at shallow depth with a limited overburden.

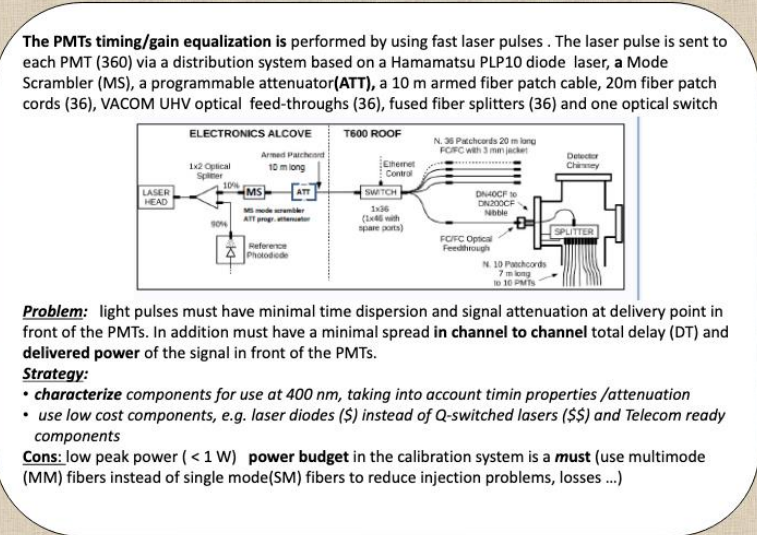
The PMTs timing/gain equalization is performed by using fast laser pulses . The laser pulse is sent to each PMT (360) via a distribution system based on a Hamamatsu PLP10 diode laser, a Mode Scrambler (MS), a programmable attenuator(ATT), a 10 m armed fiber patch cable, 20m fiber patch cords (36), VACOM UHV optical feed-throughs (36), fused fiber splitters (36) and one optical switch

Problem: light pulses must have minimal time dispersion and signal attenuation at delivery point in front of the PMTs. In addition must have a minimal spread in **channel to channel** total delay (DT) and **delivered power** of the signal in front of the PMTs.

Strategy:

- **characterize** components for use at 400 nm, taking into account timin properties /attenuation
- use low cost components, e.g. laser diodes (\$) instead of Q-switched lasers (\$\$) and Telecom ready components

Cons: low peak power (< 1 W) **power budget** in the calibration system is a **must** (use multimode (MM) fibers instead of single mode(SM) fibers to reduce injection problems, losses ...)



The PMTs timing/gain equalization is performed by using fast laser pulses . The laser pulse is sent to each PMT (360) via a distribution system based on a Hamamatsu PLP10 diode laser, a Mode Scrambler (MS), a programmable attenuator(ATT), a 10 m armed fiber patch cable, 20m fiber patch cords (36), VACOM UHV optical feed-throughs (36), fused fiber splitters (36) and one optical switch

Problem: light pulses must have minimal time dispersion and signal attenuation at delivery point in front of the PMTs. In addition must have a minimal spread in **channel to channel** total delay (DT) and **delivered power** of the signal in front of the PMTs.

Strategy:

- **characterize** components for use at 400 nm, taking into account timin properties /attenuation
- use low cost components, e.g. laser diodes (\$) instead of Q-switched lasers (\$\$) and Telecom ready components

Cons: low peak power (< 1 W) **power budget** in the calibration system is a **must** (use multimode (MM) fibers instead of single mode(SM) fibers to reduce injection problems, losses ...)

The PMTs timing/gain equalization is performed by using fast laser pulses . The laser pulse is sent to each PMT (360) via a distribution system based on a Hamamatsu PLP10 diode laser, a Mode Scrambler (MS), a programmable attenuator(ATT), a 10 m armed fiber patch cable, 20m fiber patch cords (36), VACOM UHV optical feed-throughs (36), fused fiber splitters (36) and one optical switch

Problem: light pulses must have minimal time dispersion and signal attenuation at delivery point in front of the PMTs. In addition must have a minimal spread in **channel to channel** total delay (DT) and **delivered power** of the signal in front of the PMTs.

Strategy:

- **characterize** components for use at 400 nm, taking into account timin properties /attenuation
- use low cost components, e.g. laser diodes (\$) instead of Q-switched lasers (\$\$) and Telecom ready components

Cons: low peak power (< 1 W) **power budget** in the calibration system is a **must** (use multimode (MM) fibers instead of single mode(SM) fibers to reduce injection problems, losses ...)

- The PMTs timing/gain equalization** is performed by using fast laser pulses . The laser pulse is sent to each PMT (360) via a distribution system based on a Hamamatsu PLP10 diode laser, a Mode Scrambler (MS), a programmable attenuator(ATT), a 10 m armed fiber patch cable, 20m fiber patch cords (36), VACOM UHV optical feed-throughs (36), fused fiber splitters (36) and one optical switch
-
- Problem:** light pulses must have minimal time dispersion and signal attenuation at delivery point in front of the PMTs. In addition must have a minimal spread in **channel to channel** total delay (DT) and **delivered power** of the signal in front of the PMTs.
- Strategy:**
- **characterize** components for use at 400 nm, taking into account timin properties /attenuation
 - use low cost components, e.g. laser diodes (\$) instead of Q-switched lasers (\$\$) and Telecom ready components
- Cons:** low peak power (< 1 W) **power budget** in the calibration system is a **must** (use multimode (MM) fibers instead of single mode(SM) fibers to reduce injection problems, losses ...)

The PMTs timing/gain equalization is performed by using fast laser pulses . The laser pulse is sent to each PMT (360) via a distribution system based on a Hamamatsu PLP10 diode laser, a Mode Scrambler (MS), a programmable attenuator(ATT), a 10 m armed fiber patch cable, 20m fiber patch cords (36), VACOM UHV optical feed-throughs (36), fused fiber splitters (36) and one optical switch

Problem: light pulses must have minimal time dispersion and signal attenuation at delivery point in front of the PMTs. In addition must have a minimal spread in **channel to channel** total delay (DT) and **delivered power** of the signal in front of the PMTs.

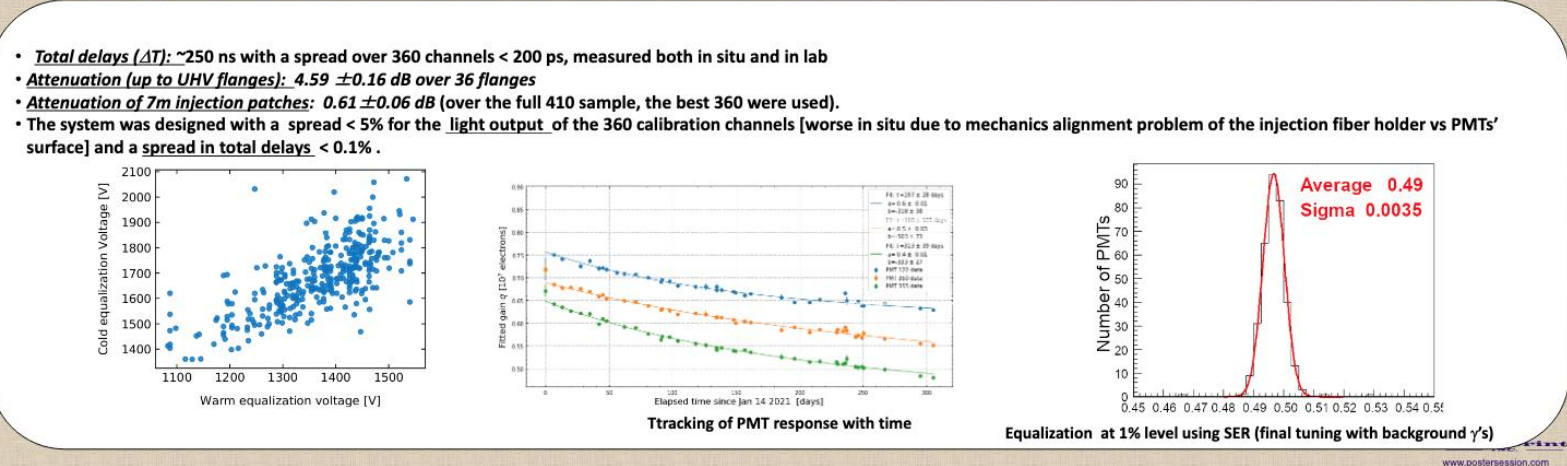
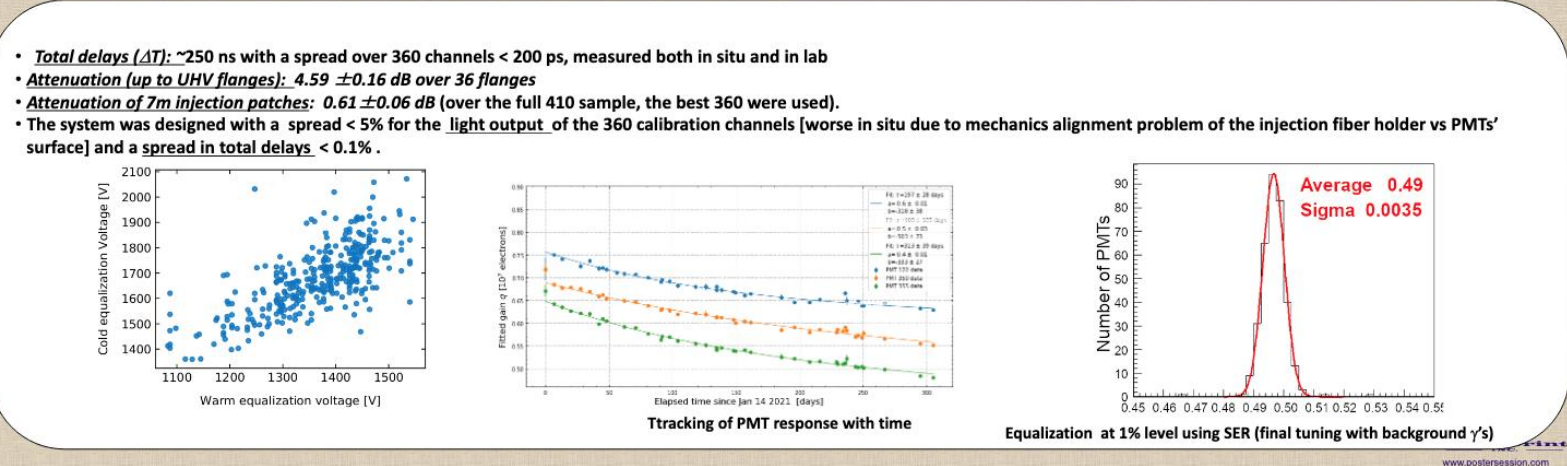
Strategy:

- **characterize** components for use at 400 nm, taking into account **timin** properties /attenuation
- use **low cost** components, e.g. laser diodes (\$) instead of Q-switched lasers (\$\$) and Telecom ready components

Cons: low peak power (< 1 W) **power budget** in the calibration system is a **must** (use multimode (MM) fibers instead of single mode(SM) fibers to reduce injection problems, losses ...)

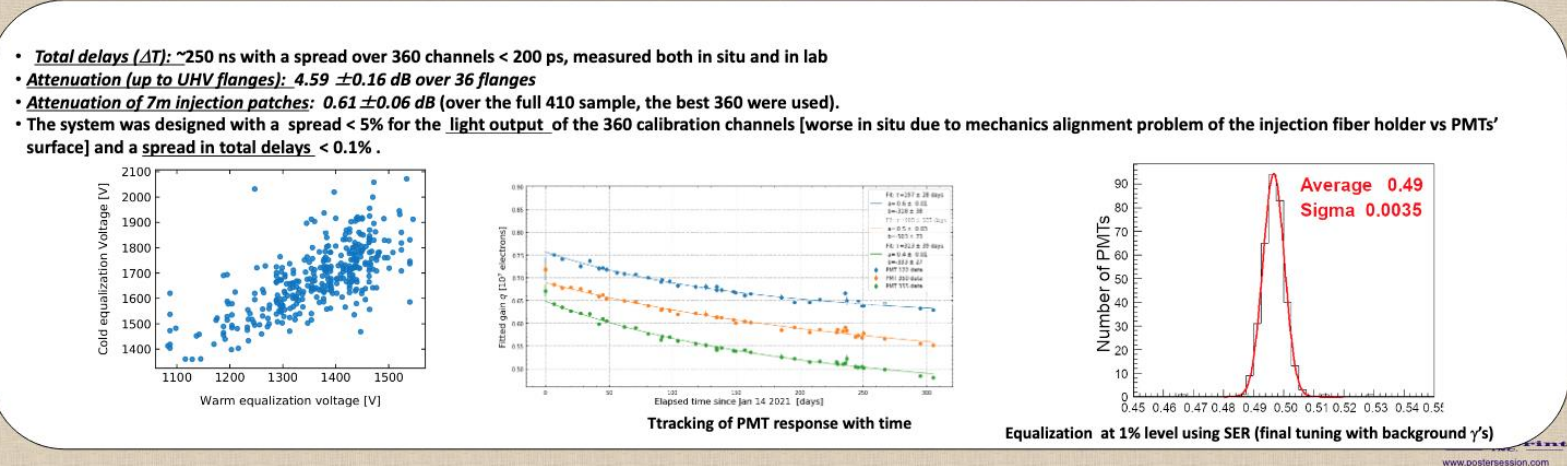
- **Total delays (ΔT):** ~250 ns with a spread over 360 channels < 200 ps, measured both in situ and in lab
 - **Attenuation (up to UHV flanges):** 4.59 ± 0.16 dB over 36 flanges
 - **Attenuation of 7m injection patches:** 0.61 ± 0.06 dB (over the full 410 sample, the best 360 were used).
 - The system was designed with a spread < 5% for the light output of the 360 calibration channels [worse in situ due to mechanics alignment problem of the injection fiber holder vs PMTs' surface] and a spread in total delays < 0.1%.

The figure consists of three subplots. The left plot is a scatter plot of 'Cold equalization voltage [V]' (y-axis, 1400 to 2100) versus 'Warm equalization voltage [V]' (x-axis, 1100 to 1500), showing a positive correlation. The middle plot is a line graph titled 'Tracking of PMT response with time', showing 'Fitted gain $\times 10^4$ electrons' (y-axis, 0.50 to 0.90) versus 'Elapsed time since Jan 14 2021 [days]' (x-axis, 0 to 300). It includes data for three PMT types (PMT 177, PMT 202, PMT 177) and their respective fits. The right plot is a histogram of 'Number of PMTs' (y-axis, 0 to 90) versus 'Equalization at 1% level using SER (final tuning with background γ 's)' (x-axis, 0.45 to 0.55). The histogram is overlaid with a red Gaussian fit curve, with the text 'Average 0.49' and 'Sigma 0.0035' indicating the fit parameters.



- **Total delays (ΔT):** ~250 ns with a spread over 360 channels < 200 ps, measured both in situ and in lab
- **Attenuation (up to UHV flanges):** 4.59 ± 0.16 dB over 36 flanges
- **Attenuation of 7m injection patches:** 0.61 ± 0.06 dB (over the full 410 sample, the best 360 were used).
- The system was designed with a spread < 5% for the light output of the 360 calibration channels [worse in situ due to mechanics alignment problem of the injection fiber holder vs PMTs' surface] and a spread in total delays < 0.1%.

The figure consists of three subplots. The left plot is a scatter plot of 'Cold equalization voltage [V]' (y-axis, 1400 to 2100) versus 'Warm equalization voltage [V]' (x-axis, 1100 to 1500), showing a positive correlation with blue data points. The middle plot is a line graph titled 'Tracking of PMT response with time' showing 'Fitted gain g [10⁴ electrons]' (y-axis, 0.50 to 0.90) versus 'Elapsed time since Jan 14 2021 [days]' (x-axis, 0 to 300). It includes four data series: F4 (blue circles), F7 (orange squares), F6 (green triangles), and F5 (red diamonds), each with a corresponding fitted line. The right plot is a histogram titled 'Equalization at 1% level using SER (final tuning with background γ 's)' showing the 'Number of PMTs' (y-axis, 0 to 90) versus a value (x-axis, 0.45 to 0.55). The histogram is overlaid with a red Gaussian fit curve. Text on the plot indicates 'Average 0.49' and 'Sigma 0.0035'.



- **Total delays (ΔT):** ~250 ns with a spread over 360 channels < 200 ps, measured both in situ and in lab
- **Attenuation (up to UHV flanges):** 4.59 ± 0.16 dB over 36 flanges
- **Attenuation of 7m injection patches:** 0.61 ± 0.06 dB (over the full 410 sample, the best 360 were used).
- The system was designed with a spread < 5% for the light output of the 360 calibration channels [worse in situ due to mechanics alignment problem of the injection fiber holder vs PMTs' surface] and a spread in total delays < 0.1%.



Carlo Fiorini



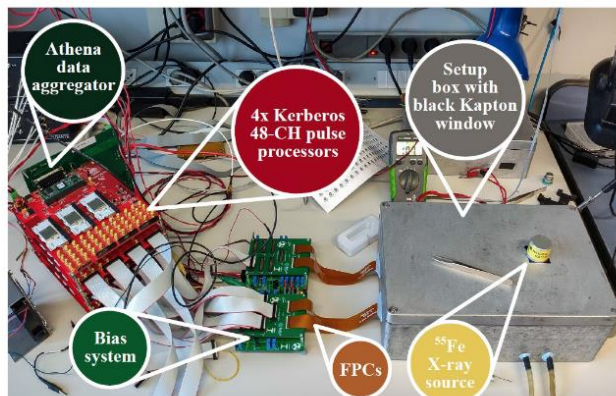
The TRISTAN Detection Module: a 166-Pixel Monolithic SDD Array for Beta Spectroscopy



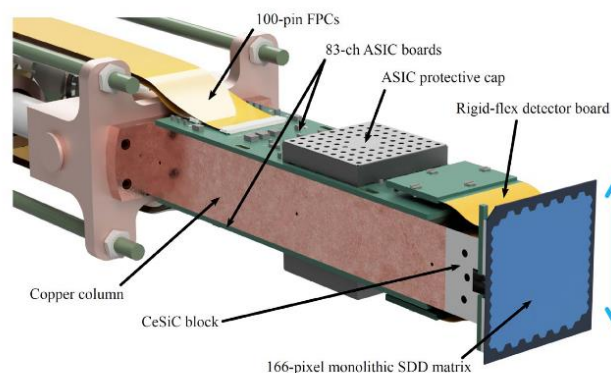
M. Carminati M. Gugiatti D. Siegmann K. Urban P. King F. Edzards P. Lechner S. Mertens and C. Fiorini

Goal: look for keV **sterile neutrino** in alterations of ^3H beta spectrum in KATRIN

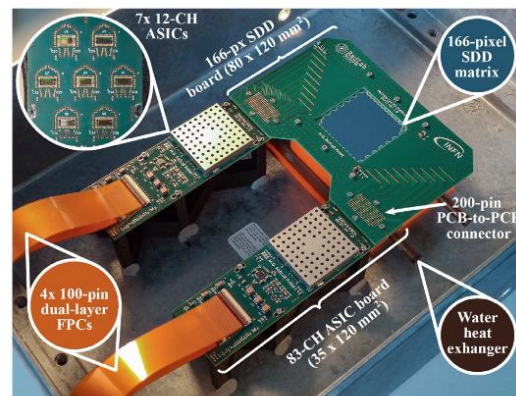
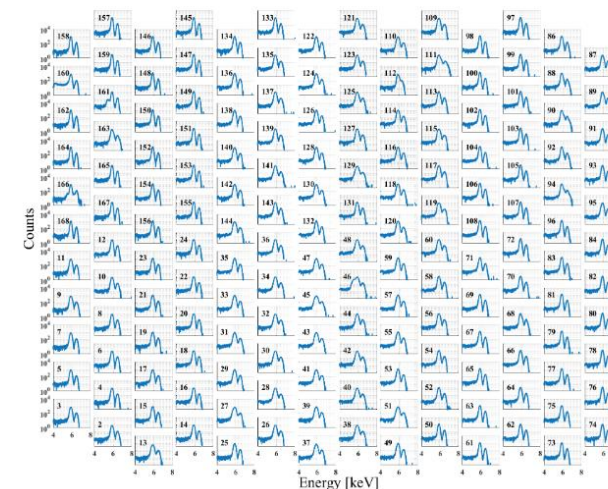
- 166 pixel integrated JFET SDD
- Integrated CSA (Ettore 12-ch)
- Integrated shapers (SFERA 16-ch)
- 192-ch DAQ (Athena)
- **High density**, low crosstalk
- Already commissioned 47 pixel
- Characterized with X-rays and e^-



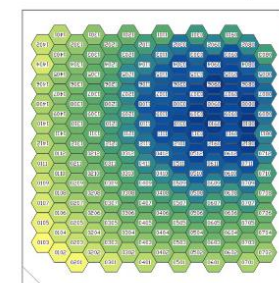
Compact Detection Module



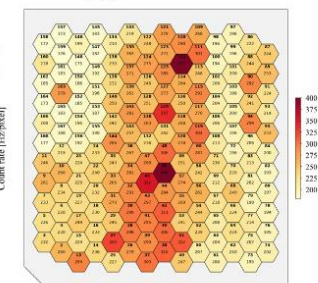
166 Simultaneous Spectra



Counts Map



Energy Resolution



Neutrino Physics and Astronomy

UHE Neutrino sources, Mass measurements

PMTs, Solid state devices, Transition Edge Sensors, Nobel liquids



Baikal-GVD

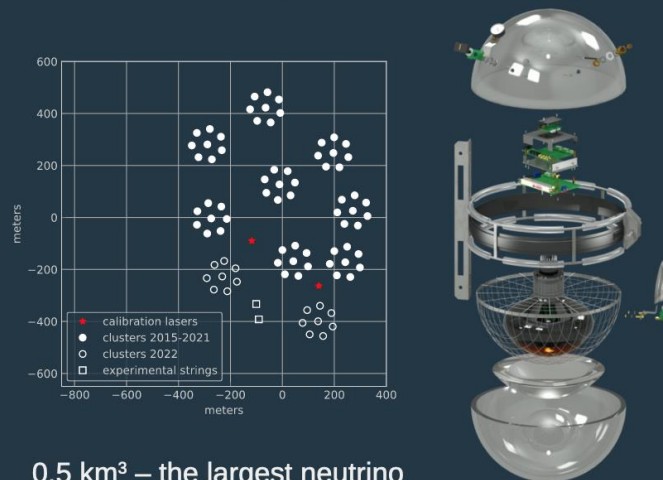
Neutrino Telescope

Gigaton
Volume
Detector

a novel tool for neutrino astronomy

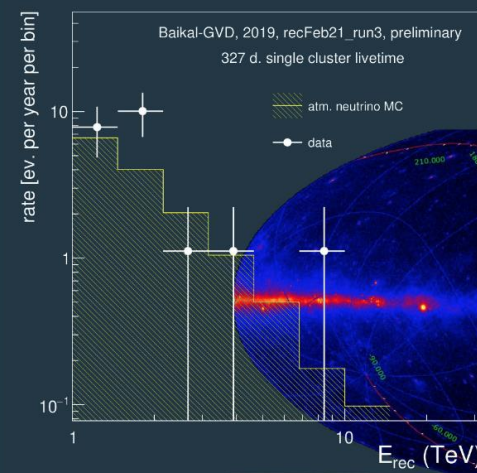
Yury Malyshkin, on behalf of
the Baikal-GVD collaboration

Design and deployment status

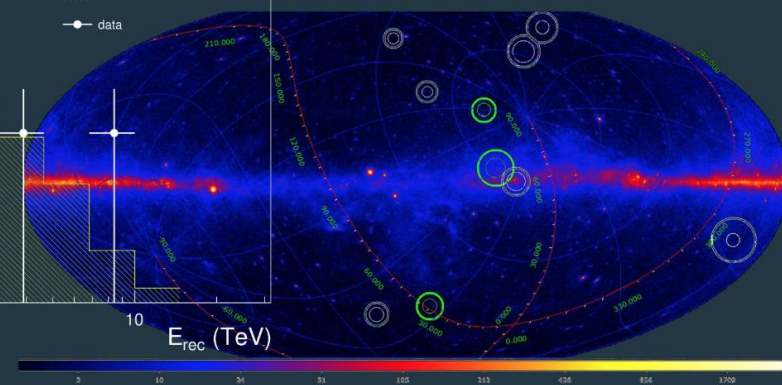


0.5 km³ – the largest neutrino
telescope in the northern
hemisphere (as of 2022)

Selected results



- First up-going track-like neutrino events
- First cascade-like astrophysical neutrino candidates





Overview of JUNO-TAO Detector

Claudio Lombardo on behalf of the JUNO collaboration

Measure reactor anti-neutrino spectrum with high resolution

- provide **model-independent reference for JUNO**
- benchmark to **test nuclear databases**
- provides increased reliability in measured **isotopic antineutrino yields**
- improve nuclear physics **knowledge of neutron-rich isotopes**
- shed light on **reactor spectrum anomaly** (5 MeV bump)
- searching for **light sterile neutrinos** with a mass ~ 1 eV
- $\sim 36 \times$ JUNO statistics

TAO Design Features:

- **2.6 ton Gd-LS** as target material (1 ton fiducial mass)
- Detector placed at **30 m distance** from a **4.6 GW_{th}** reactor core
- **10 m² SiPM**, **HPK 4x8 arrays**, with **50% PDE**, **Coverage: > 95%**
- **SiPMs and LS cooled down to -50 °C**

Expected Performance:

- ~ 4500 p.e. / MeV collected charge
- Energy Resolution: $< 2\% / \sqrt{E[\text{MeV}]}$

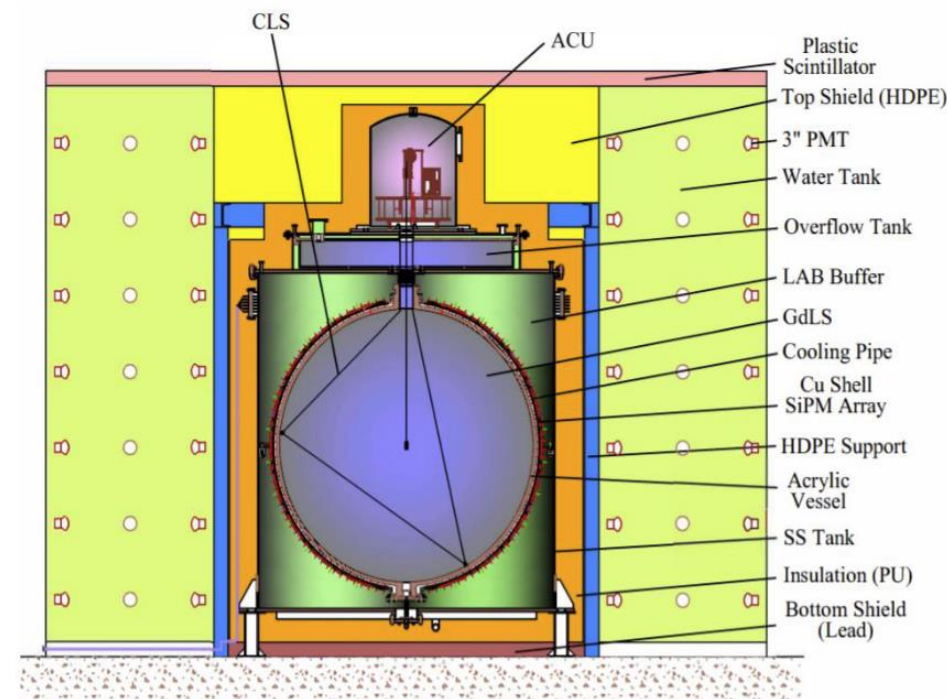
Calibration system

- **ACU (Automated Calibration Unit)**, can deploy 3 different sources inside the LS: an ultraviolet (UV) light source, a ⁶⁸Ge source and a combined source that contains multiple gamma sources and one neutron source
- **CLS (Cable Loop System)**, can deploy one source off-axis

Veto & Shielding

- **Top Plastic Scintillator**
- **Water Tank + Passive Shielding**

Planned to be online in 2023





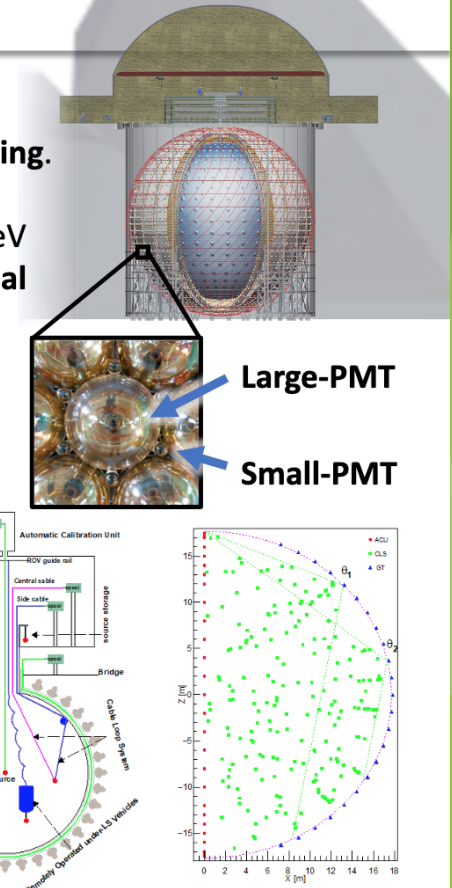
Andrea Serafini



JUNO Calibration: hardware and strategy

A. Serafini on behalf of the JUNO collaboration

- The Jiangmen Underground Neutrino Observatory (**JUNO**) is a neutrino medium baseline experiment under construction in China aiming at the determination of **neutrino mass ordering**.
- To reach its desiderata, JUNO must reach an **unprecedented energy resolution** of 3% at 1 MeV and **energy-scale systematics** below 1%. To fulfill these requirements, JUNO will feature a **dual calorimetry system** consisting of **17612 20" Large-PMTs** and **25600 3" Small-PMTs**.
- As at reactor antineutrinos' energies (<10 MeV) the Small-PMTs operate in linear regime, they can be used as a **calibration reference** for channel-wise Large-PMTs non-linearities.
- In order to accurately **characterize the detector response**, a **multiple-source campaign** relying on a specifically designed **calibration system** has been developed.
- The proposed strategy consisting in the deployment of radioactive sources to 250 different locations will enable a complete **characterization of detector non-uniformities**, permitting the characterization of the **energy resolution** and energy-related **non-linearities**.





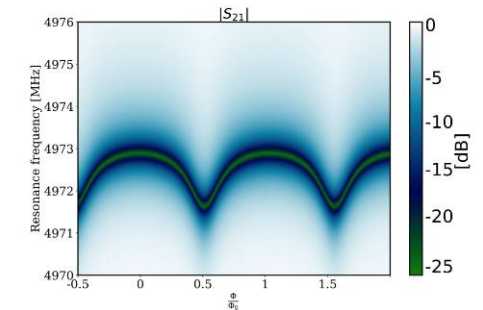
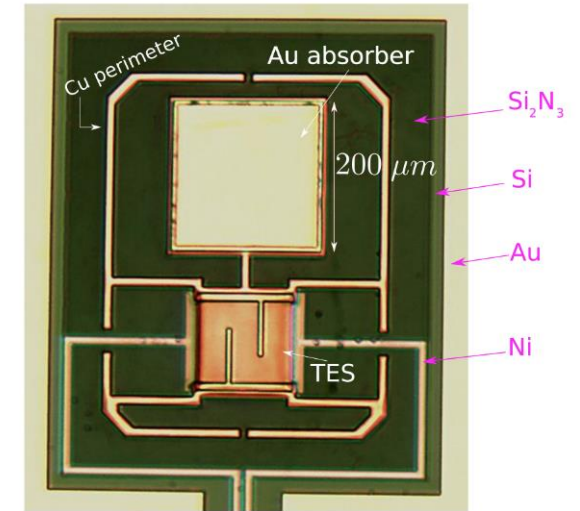
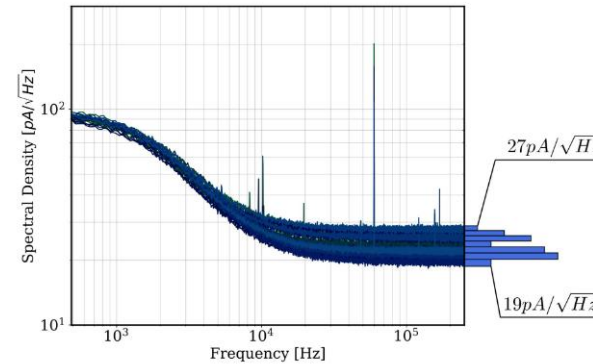
Matteo Borghesi

Toward the first neutrino mass measurement of HOLMES

M. Borghesi, on behalf of the HOLMES collaboration

HOLMES goal: prove the feasibility of the calorimetric approach for a neutrino mass measurement, using Transition Edge Sensors LTD.

- TES array fabrication (almost) complete!
- First 32 channels multiplexed readout
- Background estimation



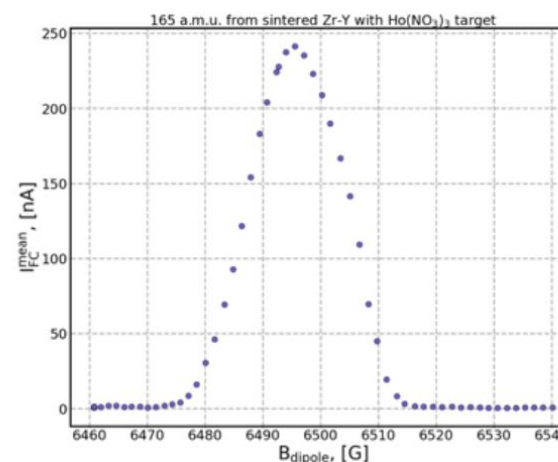
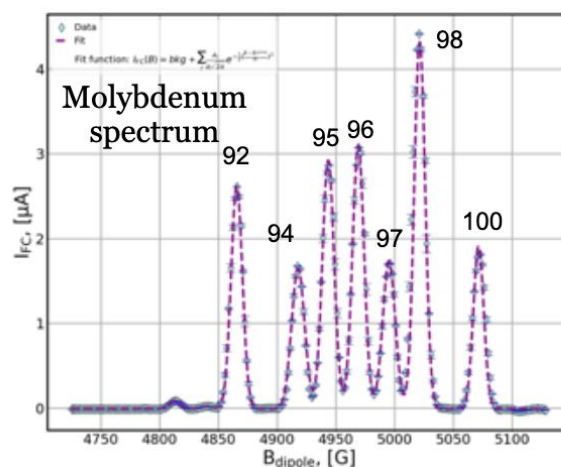


Matteo De Gerone

Development and commissioning of the ion implanter for the **HOLMES** experiment.

M. De Gerone on behalf of the HOLMES collaboration

- A beam line for implantation of ^{163}Ho atoms inside cryogenic micro-calorimeter for direct neutrino mass measurement by EC decay end-point investigation has been developed in Genova.
- The machine is calibrated by measuring reference spectra (Ar, Mo, Cu)
- R&D dedicated to identify the best way to embed Ho in ion source target
- First results with sinter-based (Zr/Y) target + ^{165}Ho showed beam current of O(200nA) @165 a.m.u.





Jacopo Dalmasson

L Gottardi & R. Caputo, Poster Overview

Assembly and characterization of a large area SiPM in Liquid Xenon Time Projection Chamber (LXe TPC)

J. Dalmasson (Stanford University) on behalf of the nEXO collaboration

The nEXO experiment

- 5 tonnes $\sim 90\%$ enriched ^{136}Xe TPC aiming to fully explore the neutrino Majorana mass in the inverted ordering
- Projected sensitivity to neutrinoless double beta decay after 10 years exposure (90% CL) $> 10^{28}\text{y}$

Three main observables are crucial to reach such result:

- Energy resolution
- Topology
- Event location

The resolution depends, among other parameters, on light collection efficiency.

Resolution [10%] vs. a/E energy resolution at Q_{EE} [%]

Resolution [10%] vs. Photon Detection Efficiency [%]

The Assembly

SiPM

Dedicated production of VUV sensitive SiPM by FBK (1cm^2 , $375\mu\text{m}$ thick)

Devices in each channel have been gain-matched based on their breakdown voltage

Ceramic Tile

Frontend Readout

- programmable voltage to each channel (SiPMs input)
- 4x8 channels DACs daisy chained (SPI controlled) controlling the different biases \rightarrow only 4 wires controlling the 32 biases
- frontend amplifier for the signal (SiPMs output)
- components modularly tested at LXe temperature

Current Setup at Stanford

Mainly developed to characterize the charge tile

Light readout features:

- 24 1cm^2 SiPMs ganged into 12 channels
- Cold frontend electronics

Need for a larger light coverage to better study energy resolution

Large Area SiPM Array Upgrade

8 fold increase in light-sensitive area:

- SiPMs epoxied and wirebonded on two ceramic tiles
- 32 channels (gang of 6 SiPMs/ch)
- Signal carried out from the cell via Kapton flex boards

Signal is amplified with 2 readout boards (16 channels each)

Digitized with a 16bit ADC (125MS/s sampling rate)

First Test in LXe

Full end-to-end test carried out in LXe

- ^{137}Cs source outside the cryostat
- V_{bias} swept from 27.4V to 32.5V
- OR threshold trigger on all 16 channels
- $6\mu\text{s}$ acquisition window



A multi-PMT photodetector system for the Hyper-Kamiokande experiment

Aurora LANGELLA*†✉

on behalf of the Hyper-Kamiokande Collaboration

* Università degli Studi di Napoli Federico II

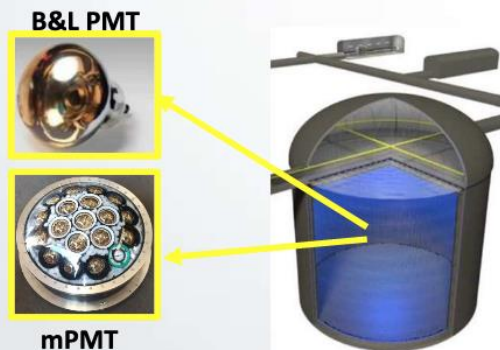
† INFN Sezione di Napoli

✉ alangella@na.infn.it



Hyper-Kamiokande (HK) is the next generation Water-Cherenkov detector with multi-purpose scientific goals in neutrino physics and non-standard physics.

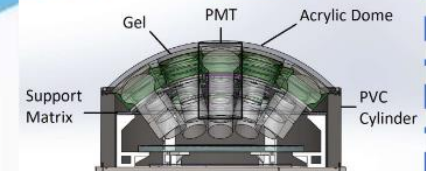
In HK Far Detector (FD) there are plans to adopt a hybrid configuration which consists of 20'' B&L PMTs and multi-PMT.



The multi-PMT (mPMT) is a novel technology for photo-detection, first designed for the KM3NeT experiment, which consists of 19 3'' PMTs and a full electronics system arranged inside a pressure vessel covered by an acrylic dome.

Advantages of mPMTs over single 20'' PMTs:

- Increased granularity;
- Overall lower dark rate;
- Better vertex resolution;
- Superior photon counting;
- Improved angular acceptance;
- Extension of dynamic range;
- Intrinsic directional sensitivity;
- Local coincidences.



Several prototypes have been realized and tested for electronics and mechanical optimization



multi-PMT electronics system for Hyper-Kamiokande

Luigi Lavitola on behalf of Hyper-Kamiokande collaboration
INFN Napoli and University of Naples Federico II
Email: lavitola@na.infn.it

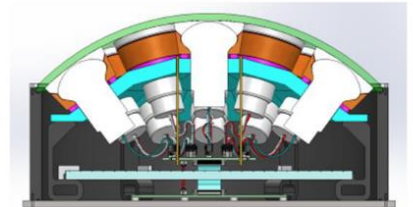
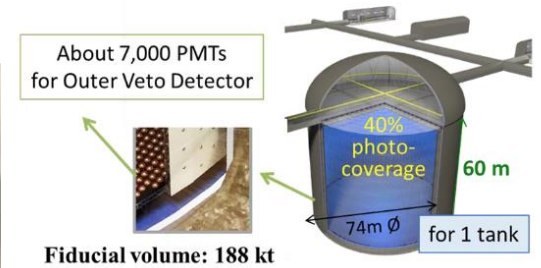


Hyper-Kamiokande



Hyper-K will benefit from the addition of the multi-PMT in the detector, introducing an intrinsic directional sensitivity, improving the timing resolution and improving the reconstruction performance, particularly for events with vertices near the photosensor plane.

- The mPMT electronics is a complete acquisition system for 19 3" PMTs in an underwater vessel with really good performance.
- HV board:
 - 3.2 mW power consumption at 1500V
 - Less than 1 % noise
 - 300 years of expected MTTF
- FE board:
 - 12 bit 2 MHz ADC, a fast amplifier for high resolution event timestamping
 - An ultra low power microprocessor running FreeRTOS
 - 40 mW of power consumption
- Main Board:
 - Redundant POE+ power supply with 87% efficiency at 4W
 - Redundant CPU to increase reliability
 - 19 individual 270 ps LSB TDC
 - 100 ns absolute timestamping
- 3.5 W of power consumption for the complete system running at 1 MHz and with the HV on on all channels



Gravitational Wave and Multimessenger Astrophysics

Near and long-term terrestrial GW detectors (~ 100 Hz), UV and IR telescopes
Interferometers (+ test masses), mirrors & coatings, solid state devices



Piero Chessa



The seismic isolation system of AdVirgo+ Phase II

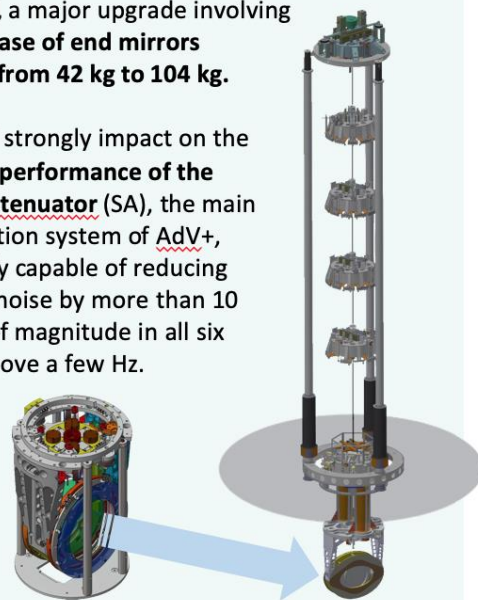
A. Basti², V. Boschi¹, P. Chessa²,
V. Dattilo³, R. Passaquieti², P. Ruggi³



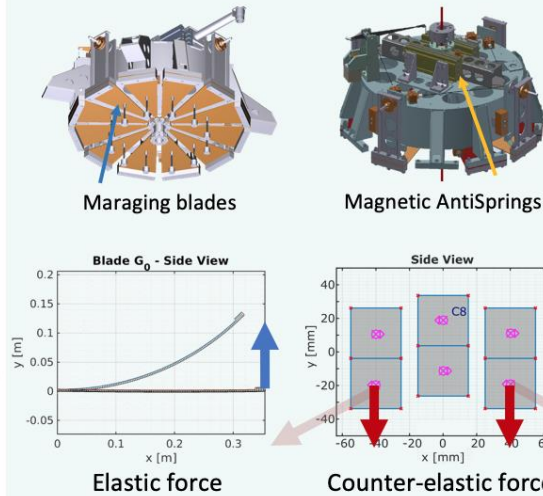
1 Istituto Nazionale di Fisica Nucleare (INFN) - 2 Università di Pisa - 3 European Gravitational Observatory

By the end of 2024, the Advanced Virgo+ (AdV+) gravitational wave detector will enter its **Phase II**, a major upgrade involving an **increase of end mirrors masses from 42 kg to 104 kg**.

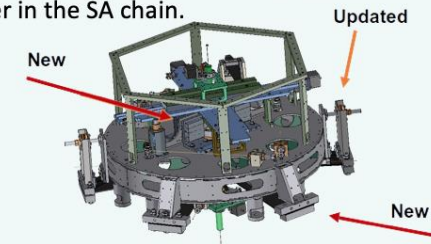
This will strongly impact on the **vertical performance of the SuperAttenuator (SA)**, the main attenuation system of AdV+, currently capable of reducing seismic noise by more than 10 orders of magnitude in all six DOFs above a few Hz.



Simulations, design activity and tests of the upgrade of the elastic (**maraging blades**) and counter-elastic components (**magnetic AntiSprings**) of the SA filters are presented.



Current studies led to upgraded blades, AntiSprings and design of **Filter 7 (F7)**, the lowest filter in the SA chain.



End SA parameters are set to **reach or exceed** the Phase II requirements.

A **prototype** of new F7 is under construction.

Filter	Load [kg]	Blades stiffness [N/m]	AS stiffness [N/m]	Freq [Hz]	Non-linearity [Phase II / I]
0	1223	108644	- 104298	0.3	1.07
1	1050	93277	- 89546	0.3	1.03
2	885	78620	- 75475	0.3	1.03
3	745	66185	- 63537	0.3	1.00
4	630	55703	- 53475	0.3	0.72
7	285	25493	- 24473	0.3	0.67



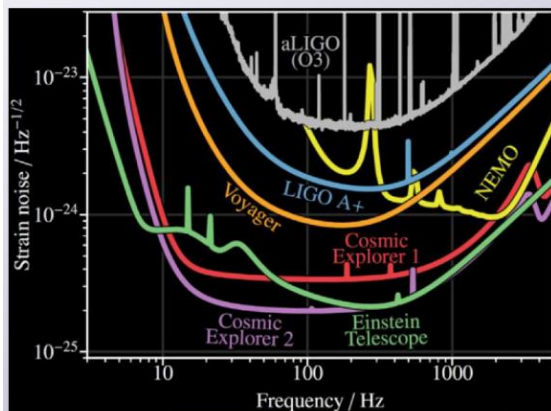
Valerio Boschi

BHETSA, a seismic isolation system for the test masses of the Einstein Telescope

Black Holes for ET Sardinia (BHETSA) is a 3-year project funded by the PRIN2020 MIUR call. Its goal is the design of a suspension system that isolates seismically the test masses of the Einstein Telescope at frequencies above 2 Hz with a height of about 10 m, similar to the one of the Virgo Superattenuator (SA). To test the new design a prototype will be constructed, tested and validated.

While based on current VIRGO SA, the mechanical solutions proposed envisaged both an upgrade of the standard filters and of the inverted pendulum pre-isolator.

Achieving detections of **low frequency gravitational waves** is crucial for the science program of the Einstein Telescope



Filter 0

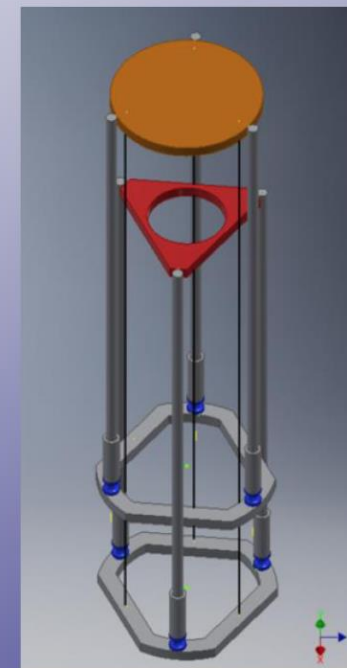
Wires

Standard Filter

Inverted Pendulum

Filter 7

Payload



The prototype will be tested in Sardinia at the **SOS Enattos** candidate site for ET





Luisa Spallino

Frost and electrostatic charge formation in mirrors of future gravitational wave detectors: mitigation strategies for two potential showstoppers



2021 15th Pisa Meeting
on Advanced Detector –
Edition 2022

L. Spallino*, M. Angelucci, and R. Cimino
LNF-INFN, Frascati (Rome) Italy
*luisa.spallino@lnf.infn.it



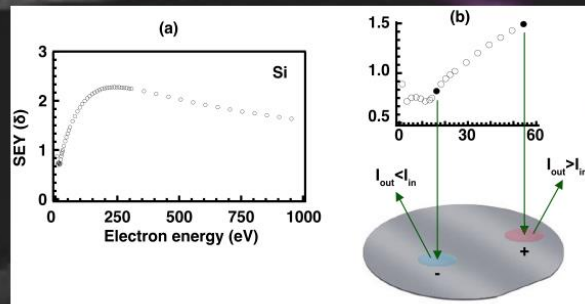
Electrostatic charging

Electrostatic charge has been shown to affect data taking already at RT. Its mitigation routinely requires mirror's long exposures to tenth of mbar of N₂ ions flux. This method cannot be applied at LT.
[L. Spallino et al., Phys. Rev. D, 105, 042003 (2022)]

Frost formation

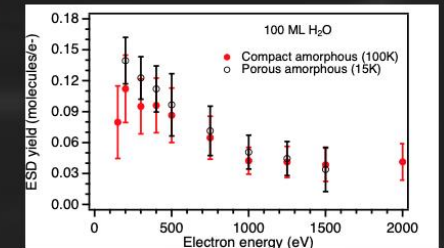
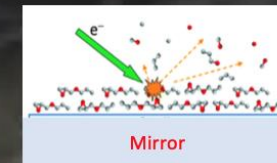
At cryogenic temperature, residual gas will condense on the mirrors' surface affecting reflectivity and inducing thermal noise.
[L. Spallino et al., Phys. Rev. D, 104, 062001 (2021)]

Electrons are shown to be able to tackle both effects synergically. Proof of principle → validation



- It is possible to tailor electron energies to induce positive or negative charge on a neutral surface

Low energy electrons irradiation can remove frost and cure electrostatic charging



- Electrons efficiently induce molecular ice nonthermal desorption, with a duration and a thermal power delivered on the surface lower in respect to thermal desorption.
- Electrons penetrate below the surface only for few nm, so that minimal effects on mirror optical quality are expected

Ultra-fast infrared detector for astronomy

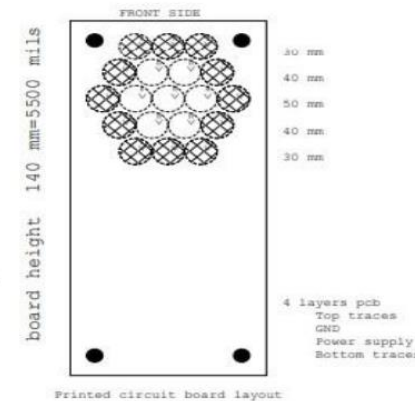


Alessandro Drago (UNI-FI & INFN/LNF), Emanuele Pace (UNI-FI),
Simone Bini, Mariangela Cestelli Guidi, Catalina Curceanu,
Augusto Marcelli (INFN/LNF), Valerio Bocci (INFN-Roma1)

- The multi-messenger astronomy, started in 2017, needs for longitudinal (temporal) more than transverse (image) detectors for telescopes in all the electromagnetic range to discover fast and slow transients synchronized with the gravitational waves.
- Experience done to detect the pulsed infrared synchrotron light in e⁺/e⁻ circular accelerator has demonstrated the feasibility to acquire mid-IR signals with rise time up to ~1 ns by single pixel HgCdTe semiconductor at room temperature.
- Design of an infrared detector for ground-based telescopes has been partially funded by INFN and it is in progress. The previous detector has been modified and upgraded for the astronomy to be able to record from ultra-fast to very slow transients and to acquire fainter and noisier signals. In phase 1, FAIRTEL will have 1 signal pixel and 1 dark pixel, in phase 2, it will have 7+12 pixels.

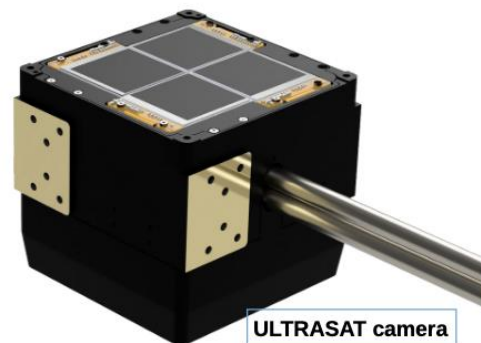


board width 70mm=2755.9mils

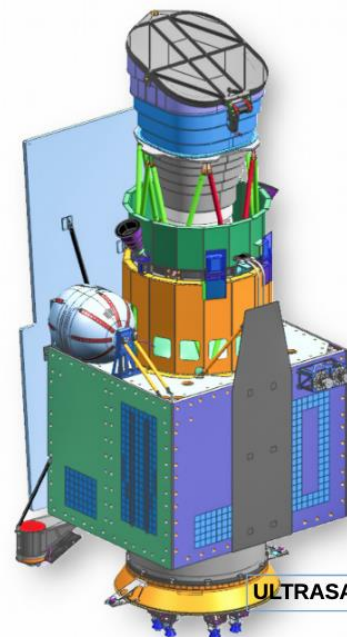


Total Ionizing Dose effects on CMOS Image Sensor for the ULTRASAT space mission

Vlad Berlea - ULTRASAT mission



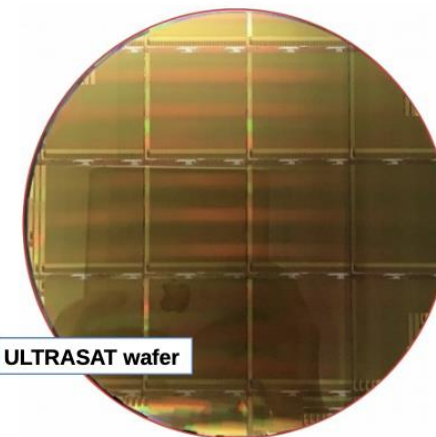
ULTRASAT camera



ULTRASAT satellite

ULTRASAT

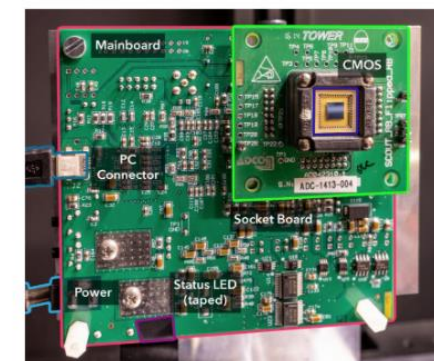
- **UltraViolet** **Transient** **Astronomical** **Satellite** is a wide-angle space telescope that will perform a deep time-resolved all-sky survey in the near-ultraviolet. The 90 Megapixel camera will operate at -70°C .
- The science objectives are the detection of counterparts to gravitational wave sources and supernovae.
- The launch is expected in early 2025 and 3 years of orbit operations are planned as a minimum. DESY will provide the UV camera, composed by the detector assembly located in the telescope focal plane and the remote electronics unit.



ULTRASAT wafer

Total Ionizing Defects on Tower test structures

- In order to predict the radiation effects on the final sensors, preliminary studies on Tower test structures (Scouts) with similar pixels have been performed.
- Both the Flight ULTRASAT sensors and the Scout test structures are 4T Back Side Illuminated Sensors, built in the Tower 180 nm architecture, with similar photo-diode geometries.
- The Total Ionizing Dose effects on the test structure pixels is presented. An important component from Random Telegraph Signal is observed.



Tower test structures



HELMHOLTZ

X-ray and Gamma-ray Telescopes

Polarization, Simulations, On-orbit performance

Mirrors, solid state devices



Luca Latronico

Enabling precise X-ray polarimetry for the IXPE space explorer



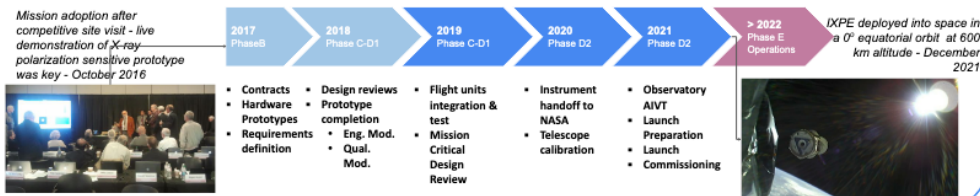
L. Latronico
INFN Torino, Via P. Giuria 1, 10125 Torino, Italy
on behalf of the IXPE Collaboration



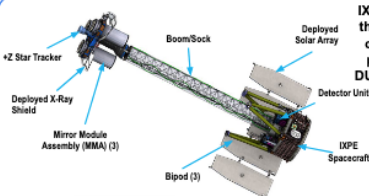
Successfully launched in December 2021, after only five years from the adoption, IXPE belongs to the NASA Explorers program, which offers frequent flight opportunities for world-class scientific investigations from space. IXPE will accomplish the first-ever survey of the polarization properties of tens of celestial X-ray sources, with percent accuracy, and within the boundaries of a small explorer program. This goal can be achieved with the use of Gas Pixel Detectors, which precisely reconstruct the sub-mm long tracks of single electrons generated by the photo-electric interactions of incoming soft X-rays. This poster summarises the most important design elements of the GPDs and of the Detector Unit housing them, the qualifications obtained for operating them onboard IXPE, and the fast-paced integration and verification cycle entirely developed in Italy to make the IXPE mission a reality.

The Mission

IXPE is a NASA Small Explorer, cost-capped at ~200M\$ with a timeline of 5 years to launch and a 2-year baseline operations



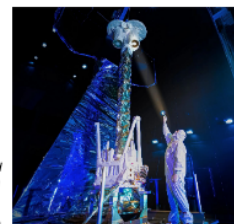
The Telescope



IXPE images X-rays in the 2-8 KeV range and measures their polarization using three identical telescopes each comprised of a Mirror Module Assembly (MMA) and a polarization sensitive Detector Unit (DU) at its focus. DU Data are handled by the Detector Service Unit (DSU).

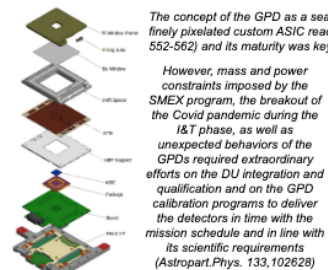
The mission is managed by Marshall Space Flight Center (MSFC), which was also responsible for the MMA fabrication, testing, and calibration.

The Italian Space Agency (ASI) delivered the Instrument, which comprises the DUs, which were designed, assembled and qualified by INFN and calibrated at INAF-IAPS, and the DSU, designed and fabricated by OHB. Ball Aerospace integrated the Observatory. Space-X launched IXPE into space and placed it on its orbit



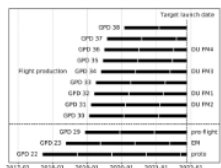
The Detector

The IXPE Gas Pixel Detectors (GPD) can reconstruct single photo-electron tracks with ~ μm resolution, thus mapping the polarization of the incident beam, with better than 20% resolution at 5.9KeV and ~1 msec typical deadline between photons. These GPDs are truly enabling a new observational window in X-ray astrophysics, as demonstrated by the first results (see A. Manfreda's talk).

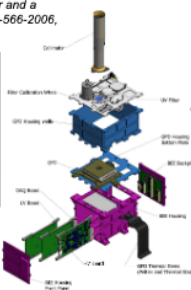


The concept of the GPD as a sealed gas cell with a Gas Electron Multiplier and a finely pixelated custom ASIC readout was conceived 15 years ago (NIM-A-566-2006, 552-562) and its maturity was key in the adoption by NASA for IXPE.

However, mass and power constraints imposed by the SMEX program, the breakout of the Covid pandemic during the I&T phase, as well as unexpected behaviors of the GPDs required extraordinary efforts on the DU integration and qualification and on the GPD calibration programs to deliver the detectors in time with the mission schedule and in line with its scientific requirements (Astropart.Phys. 133, 102628)



12 GPDs were built and calibrated equivalent to a 25 GPD-year operation



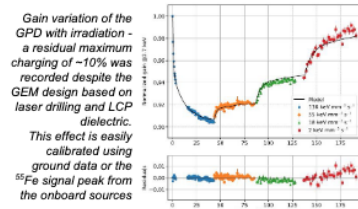
Each DU hosts the GPD with its electronics and services.

DUs were designed, assembled and qualified by INFN under the requirement to minimize their footprint and allocate three DUs on the spacecraft top deck, in order to maximize the telescope effective area and reduce systematics effects by operating three independent detectors symmetrically oriented around the target.

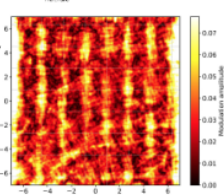
Tight constraints on the DU mass, dimensions and mechanical rigidity were applied in the design to match the capabilities of the Pegasus launcher originally foreseen in the proposal.

When Space-X won the tender, suddenly a ~10x mass and dimension margin appeared at less than one year into launch.

The additional power offered by the Falcon-9 rocket was then used to place the original IXPE design into a real equatorial orbit with minimum background and satellite drag, potentially extending the mission lifetime to more than a decade

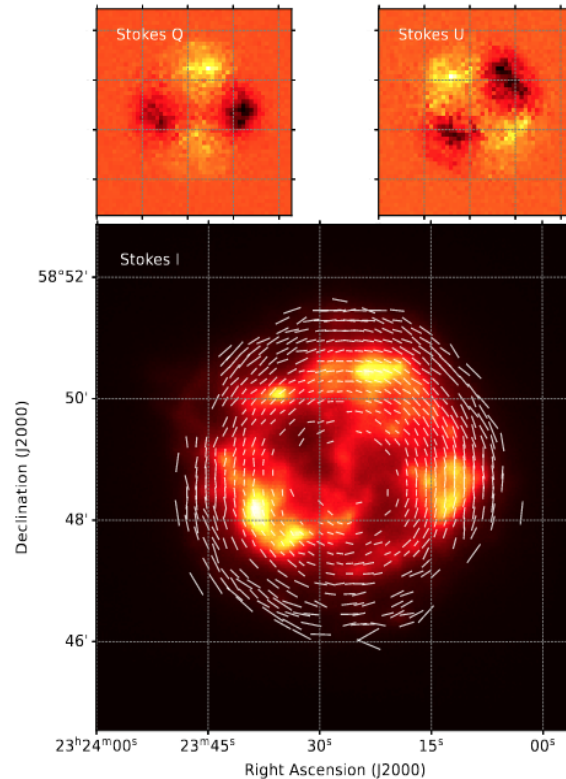


A structured ~% level modulation from unpolarized X-rays was recorded through calibrations. This effect is kept under control by dithering the satellite, effectively averaging the response across the active surface. The IXPE sensitivity to polarization is so restored to typical Minimum Detectable Polarizations of few %, opening the way to the first-ever polarization census of 10s of X-ray sources





Melissa Pesce-Rollins



ixpeobssim is a simulation framework developed for the Imaging X-ray Polarimetry Explorer (IXPE) mission. It is meant to produce fast and yet realistic observation-simulations, given as basic inputs:

- ▷ an arbitrary source model including morphological, temporal, spectral and polarimetric information;
- ▷ the response functions of the detector

The framework produces output files that can be directly fed into the standard visualization and analysis tools used by the X-ray community.

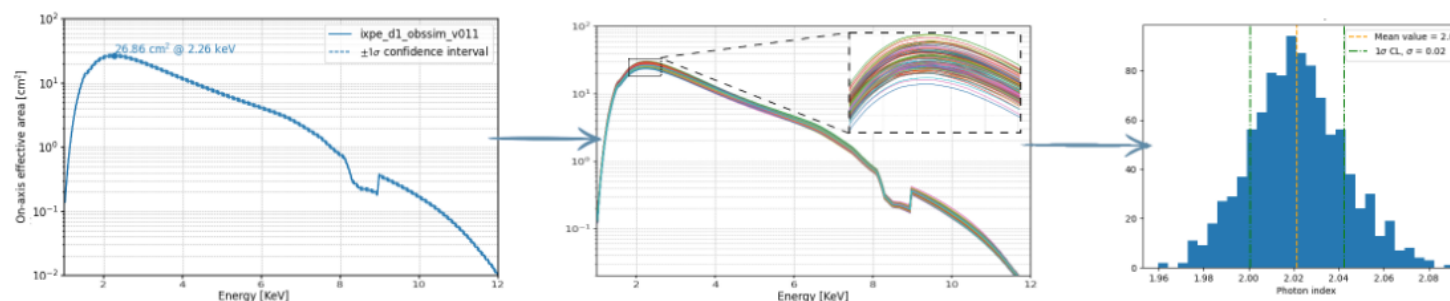
Accounting for systematic uncertainties in the Imaging X-ray Polarimetry Explorer (IXPE) detector response

Modeling of systematics

- ▷ The shapes of instrumental response functions (IRFs) have been altered to simulate the effect of systematic errors
- ▷ A simulated source has been folded with the altered IRFs to see the error induced in parameter estimation

Results

- ▷ Systematic errors are compatible with the statistical error in the polarization degree only for very bright sources.
- ▷ The systematic error largely dominates the statistical error in the Normalization and photon index for bright sources.
- ▷ Errors on the energy scale shows similar behavior and influences the polarization degree only for exceptionally bright sources, being the relevant source of uncertainty for spectral parameters.





Simone Maldera



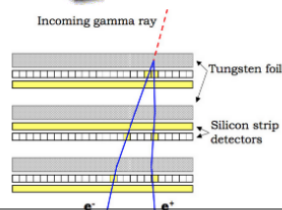
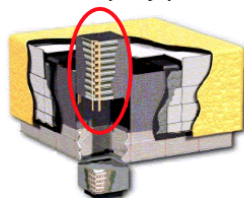
Performances of the Fermi-LAT silicon strip tracker after 14 years of operation

S. Maldera¹ on behalf of the Fermi-LAT collaboration
¹ Istituto Nazionale di Fisica Nucleare - Torino



The Fermi-LAT Tracker

The **Large Area Telescope (LAT)** is a pair-conversion γ -ray detector able to measure γ -ray photons from 30 MeV to more than 300 GeV.



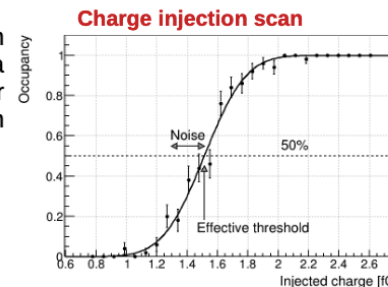
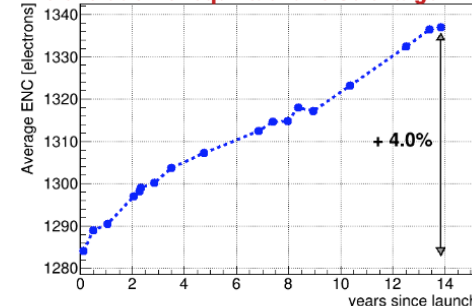
LAT Tracker

- 18 x-y detection planes of single sided silicon strip detector (SDD)
- Interleaved with tungsten foils to increase conversion probability (12 foils $0.03 X_0$ thick, 4 foils $0.18 X_0$ thick)
- 4 parallel ladders, each ladder built by connecting the strips of 4 SSD
- 400 μ m thickness, pitch of 228 μ m, 15536 strips per layer
- data stream: hit strips coordinates (digital readout) + layer OR Time over threshold (ToT)
- Self triggering (3 bi-layers hit in the same tower)

Noise performances

Noise is monitored by means of charge injection runs. For each Si strip the average occupancy as a function of the injected charge is fitted with an error function. The slope gives an estimation of the width of the underlying noise distribution.

Time evolution of equivalent noise charge

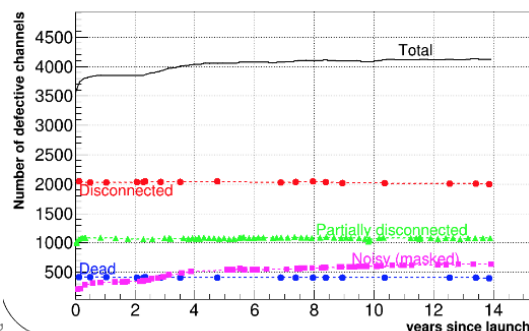


~4% increase of equivalent noise charge (ENC)

related to increased leakage current due to radiation damage

Defective channels

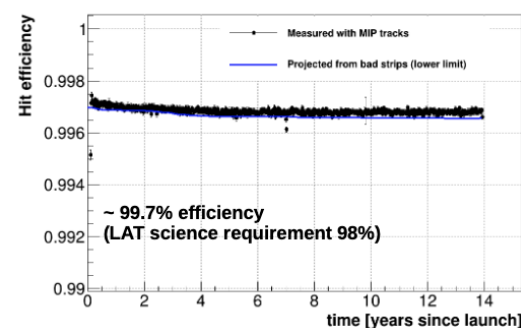
Time evolution of bad strips



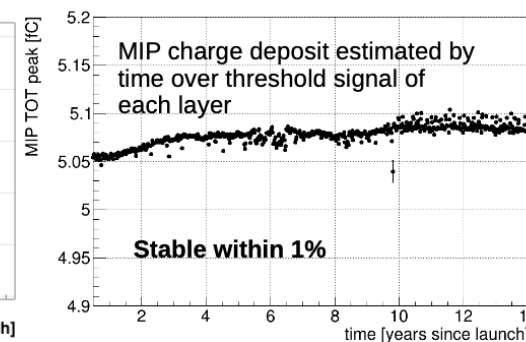
Different types of bad channels:

- Dead preamplifier.
- Disconnected: silicon strip is not physically connected to the preamplifier input. Low (~ 250 electrons) ENC.
- Noisy: noise occupancy $> 1\%$,
- Partially disconnected: one or more of the wire bonds along the ladder is defective. Intermediate noise levels.
- **3661 defective strips at launch (0.31%)**
- **4120 defective strips at present (0.46%)**

Strip hit efficiency



Mip charge monitoring



Cosmic Rays and Antimatter

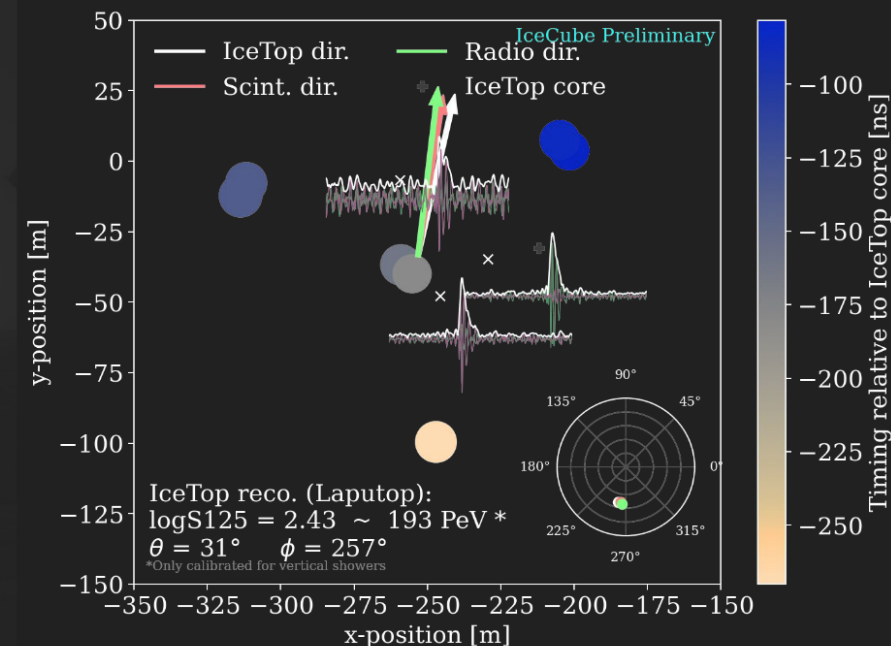
Cherenkov air showers, magnetic spectrometers,
Scintillation detectors, Radio antennae, magnets, solid state devices



Measurement of cosmic-ray air-shower radio emission with an IceCube Surface Array station

Hrvoje Dujmović for the IceCube Collaboration
15th Pisa Meeting on Advanced Detectors

- In the coming years, IceCube's cosmic-ray capabilities will be enhanced by adding scintillators and radio antennas to the surface array
- The design of the Enhancement is being tested with a prototype station deployed to the Pole in Jan. 2020
- **First cosmic-ray air-showers with the prototype station have been measured**
- Basic event reconstructions are performed on the scintillator, radio and IceTop data individually
 - The results agree with each other and the station seems to be performing as expected!
- Improved reconstructions and additional cross-checks are being worked on



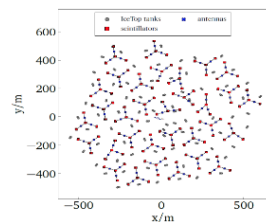


The Scintillation Detectors and its DAQ of the IceCube Surface Array Enhancement

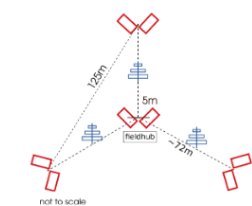
Thomas Huber for the IceCube Collaboration
- Karlsruhe Institute for Technology (KIT), Institute for Astroparticle Physics (IAP)



First full prototype station deployed early 2020



Planned layout of the full surface array enhancement



Layout of one station of the surface array enhancement



Deployed scintillation detector

- The IceCube surface array, IceTop, is foreseen to be enhanced by a hybrid detector array. Each station of the IceCube surface array enhancement will include:

- Eight Scintillation detectors,
- Three Radio antennas and
- One central data acquisition (DAQ)

- It is planned to deploy 32 of these stations in coming years to

- Lower the energy threshold for air shower detection capability,
- Improve the veto capabilities for the in-ice neutrino detection,
- Mitigate the effect of snow accumulation on the IceTop detectors,
- be able to perform multi-component observations of air showers

- These improvements of the IceCube surface array enables among others to

- Veto atmospheric neutrinos,
- Investigate the energy spectra and composition of cosmic rays in a wide energy range,
- validate hadronic interaction models



Exploring the lifetime and cosmic frontier with MATHUSLA

Cristiano Alpighiani

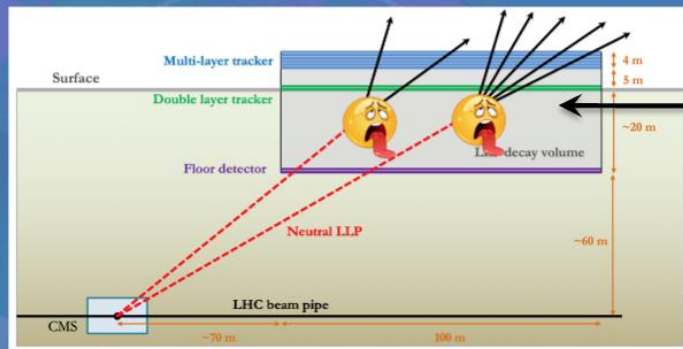
on behalf of the MATHUSLA Collaboration

15th Pisa Meeting on Advanced Detectors, La Biodola – Isola d'Elba, May 2022

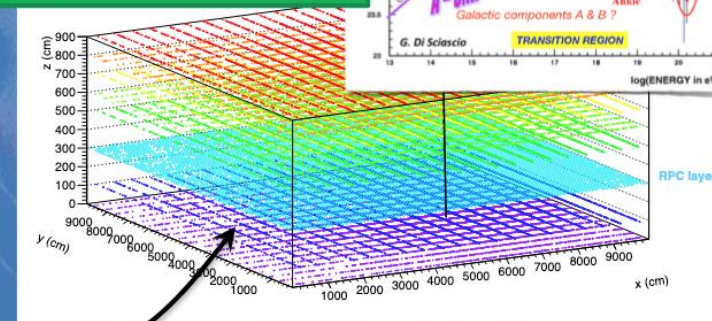
MATHUSLA

W
UNIVERSITY of
WASHINGTON

MATHUSLA: proposed detector to study neutral very long-lived particles and cosmic rays



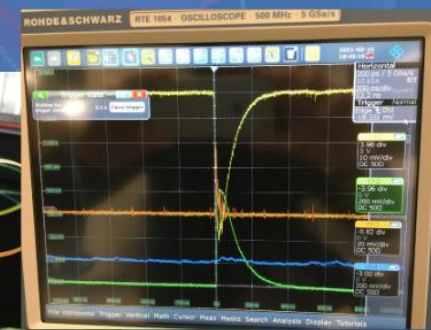
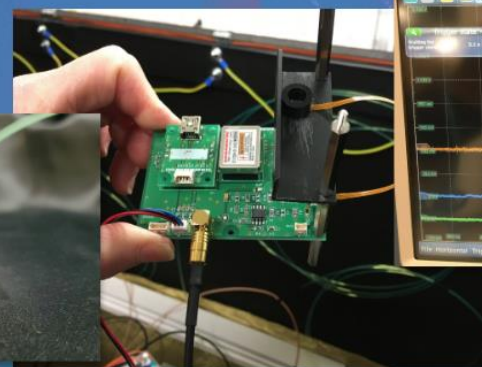
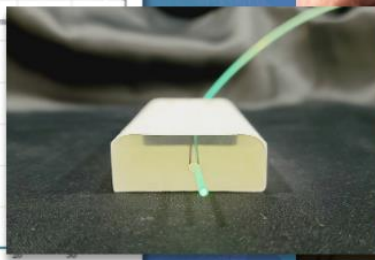
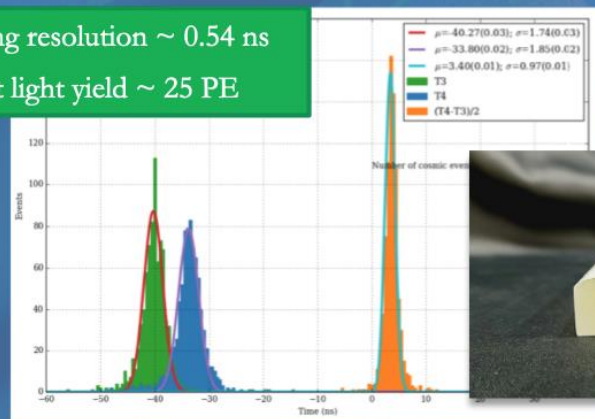
To explore the “knee” region



- Tracking: extruded scintillators + SiPM
- Ongoing R&D to study the best detector layout and technology
- Physics case for adding a layer of RPCs (for cosmic rays)

Timing resolution ~ 0.54 ns

Worst light yield ~ 25 PE





Corrado Altomare



The Plastic Scintillator Detector for the HERD experiment

HERD experiment Scientific goals:

- Cosmic Rays: precise CR spectra and mass composition (10 GeV – 3 PeV)
- Gamma – ray astronomy and transient studies (0.5 GeV – 100 TeV)
- Cosmic-ray electron and positron spectra (and anisotropies) (10 GeV – 100 TeV)
- Indirect Dark Matter searches with high sensitivity

The Plastic Scintillator Detector (PSD):

- Trigger of low energy gamma-ray events from 0.5 to 10 GeV.
- Offline high energy gamma-ray identification
- Redundant charge measurements of cosmic ray nuclei.

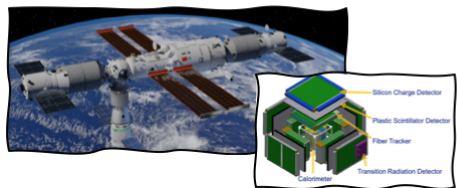


Fig.1 LEFT: rendering of the Tiangong Space Station. RIGHT: Scheme of HERD facility with the five sub-detectors. From the innermost to the outermost: CALO, FIT, PSD, SCD and TRD.

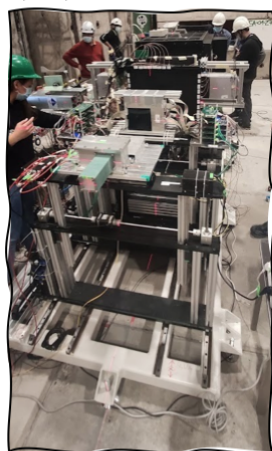


Fig.2 HERD full sub-detectors test during a CERN 2021 beam test campaign.

PSD geometry	Description	PRO	CONS
TILE	Two layer of tiles to increase nuclei identification power	High segmentation reduces back-splash effect	Higher number of readout channels
BAR	Two layer, one per view, each layer made by two staggered sub layers	Fewer readout channels	Higher back-splash contamination

2021 CERN beam test campaign:

- SiPMs and Citiroc readout
- Different plastic scintillator tested
- PSD Tiles and Bars geometry tested
- 10 GeV pions, protons and 100 GeV electrons used

Result highlights:

- Useful data to understand noise contamination.
- Geometry final decision making.

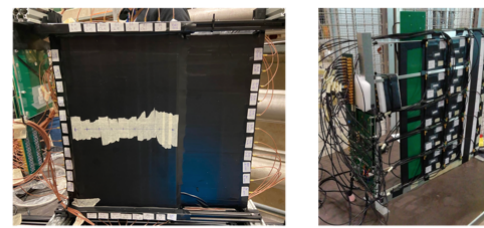


Fig.3 (a) The bar PSD prototype (b) The tile PSD prototype.

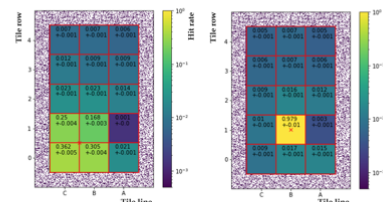


Fig.4 Fraction of events acquired with respect to the number of main triggers for 10 GeV pions beam. LEFT: the beam is centered at the intersection of 4 tiles. RIGHT: the beam impinges in the center of tile B1.

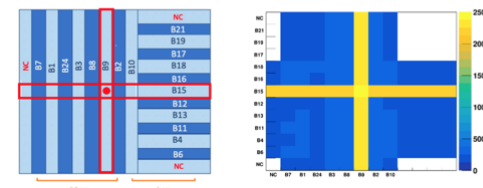


Fig.5 LEFT: Prototype layout with beam (red dot) centered in bars B9 and B15. RIGHT: The hit map reconstructed from experimental data collected with proton beam, confirming that most of the hits are detected by these 2 bars.

Corrado Altomare - for the HERD collaboration

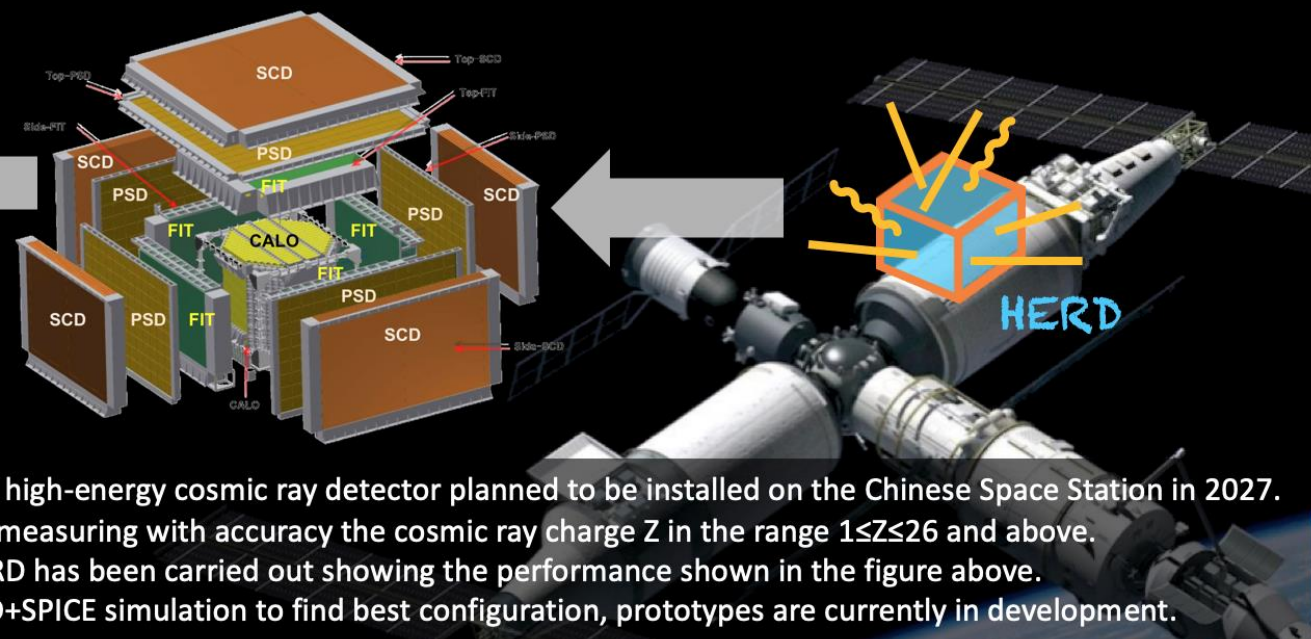
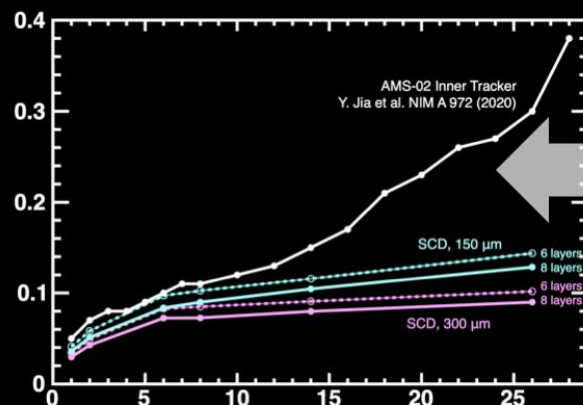


Matteo Duranti

The Silicon Charge Detector (SCD) of the High Energy Cosmic Radiation Detection facility (HERD)

M. Duranti¹ and A. Oliva² on behalf of the HERD Collaboration

¹INFN Sez. di Perugia, ²INFN Sez. di Bologna



- The HERD facility is a large-field-of-view and high-energy cosmic ray detector planned to be installed on the Chinese Space Station in 2027.
- The SCD is a specialised HERD sub-detector measuring with accuracy the cosmic ray charge Z in the range $1 \leq Z \leq 26$ and above.
- A complete simulation of the SCD in the HERD has been carried out showing the performance shown in the figure above.
- Silicon sensors have been studied with TCAD+SPICE simulation to find best configuration, prototypes are currently in development.

Frontier Detectors for Frontier Physics
15th Pisa Meeting on Advanced Detectors
22–28 May 2022



Institute of High Energy Physics
Chinese Academy of Sciences



Massimo Rossella

A tile prototype of the Plastic Scintillator Detector for HERD based on long Printed Circuit Board: design and test with ion beams at CNAO

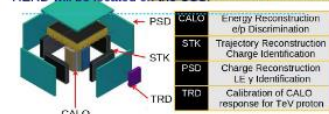
M. Rossella (INFN Pavia) paolo.cattaneo@pv.infn.it on behalf of HERD collaboration



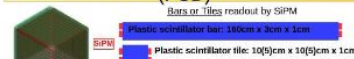
HERD detector and requirements

σ_{M}	0.1° @ 10 GeV	σ_{E}	10 GeV - 100 TeV	σ_{Nuclear}	30 GeV - 3 PeV
Z	1 - 28	Energy Range	10 GeV - 100 TeV		
σ_{p}	0.1 - 0.15 e	Energy resolution	1% @ 200 GeV		20% @ 100 GeV - 1 PeV
ϕ/θ	10°	Effective area	> 3 m² @ 200 GeV		> 2 m² @ 100 TeV

HERD will be located on



HERD Plastic Scintillator Detector (PSD)



PSD Layers

- 1 Top XY
- 4 Lateral XY
- 1 Bottom X

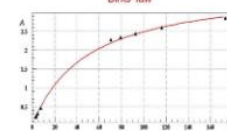
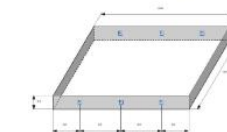
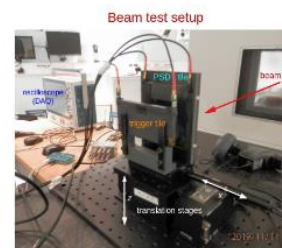
Advantages
Lower number of readout channels
Simpler mechanics
Better ID of backscattered particles
More powerful trigger

The correct identification of backscattered particles is crucial to avoid:

- charge misreconstruction in case of incident charged particles
- self veto in case of incident γ

Beam Test 2019-2020

Test scintillator tile read out by 3+3 Hamamatsu S12572 SiPM (3x3 mm²)



The correlation between the signal amplitude and the dE/dx (p^2/p^3) is well fitted with a Birks' law

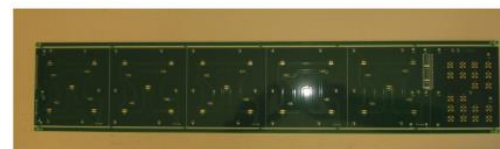
$$A = P_1 \frac{dE/dx}{1 + P_2 dE/dx}$$

$$P_1 = 0.0796$$

$$P_2 = 0.0204$$

Beam Test 2021 The 50 cm long PCB

The PCB 50 cm long PCB read by 5 SiPM 3x3 mm² and 4 1.3x1.3 mm².

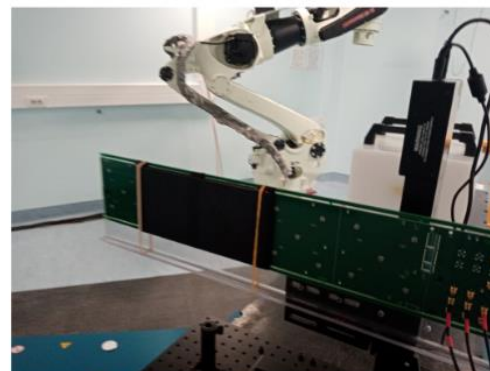
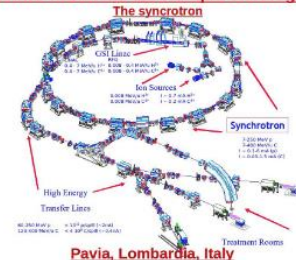


Beam test of tile prototype

CNAO provides low energy ion beams (p,C)




Centro nazionale adroterapia oncologica






Matteo Duranti

L Gottardi & R. Caputo, Poster Overview



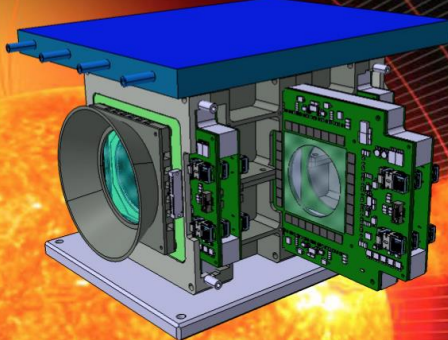
Horizon 2020
European Union Funding
for Research & Innovation

Frontier Detectors for Frontier Physics
15th Pisa Meeting on Advanced Detectors
22–28 May 2022



PAN
Penetrating Particle Analyzer

Development of a Penetrating particle ANalyzer for high energy radiation measurements in deep space and interplanetary missions
M. Duranti - INFN Sez. Perugia on behalf of the PAN collaboration



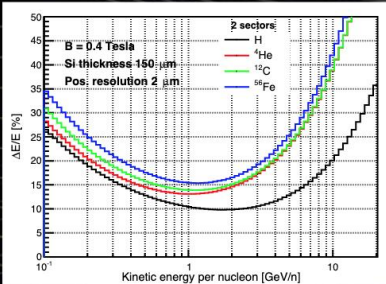
Mini.PAN Demonstrator

Mini.PAN is funded by EC as a technology demonstrator

- Max 8 kg
- 20 W
- 2 Sectors with smaller dimensions with the same instrumentation (ToF, pixel, strip)
- Mini.PAN is suitable for space weather and planetary radiation measurements




Mini.PAN active detection elements: TOF, PIXEL, Strip-X, Strip-Y





2 sectors
B = 0.4 Tesla
Si thickness 150 μ m
Pos. resolution 2 μ m


Acknowledgements: this project has received funding from the European Union's Horizon 2020 research and innovation programme under grant agreement No 862044.
Disclaimer: all views and opinions expressed on this site are those of the authors and do not necessarily reflect the official policy or position of any other agency, organization, employer, or company. In particular the European Commission is not responsible for any use that may be made of the information hereby contained.




UNIVERSITÉ DE GENÈVE


A.D. 1308
unipg
UNIVERSITÀ DEGLI STUDI DI PERUGIA



CTU
CZECH TECHNICAL UNIVERSITY IN PRAGUE



FACULTY OF ELECTRICAL ENGINEERING
UNIVERSITY OF WEST BOHEMIA



Cosmic ray physics, solar physics, space weather, planetary science
looking for flight opportunities



The Silicon Microstrip Tracker for the Mini.PAN experiment

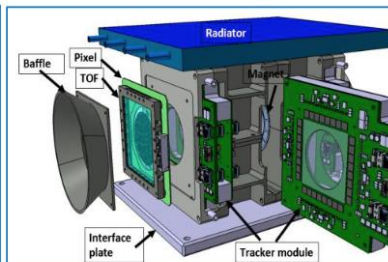
Maria Movileanu-Ionica, On behalf of PAN Collaboration (<http://www.pan-space.eu>)
INFN Sezione di Perugia, Via A.Pascoli, 06100 Perugia, Italy

A Silicon Microstrip Tracker (SMT) was built for the Penetrating-particle Analyzer demonstrator, under the framework of EU H2020 FET-OPEN grant. The SMT characteristics and construction technology are described, the quality and performances of the detector will be reported.

Mini.PAN main components:

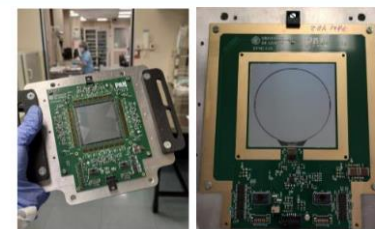
2 permanent magnets, 3 silicon tracker modules, 2 pixel detectors and 2 TOF modules.

Total dimensions: 20cm x 30cm x 20cm; Weight: max. 10kg; Total Power consumption: < 30W



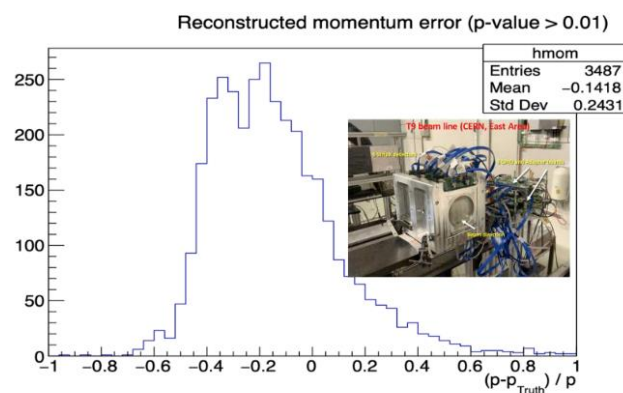
SILICON MICROSTRIP MODULE

- Two Strip-X sensors with 2048 channels readout by 32 VA1140 chips on all four sides. Fine pitch of 25μm
- One Strip-Y sensor with 128 channels readout by one VATAGP7.2 chip. Readout pitch 400μm

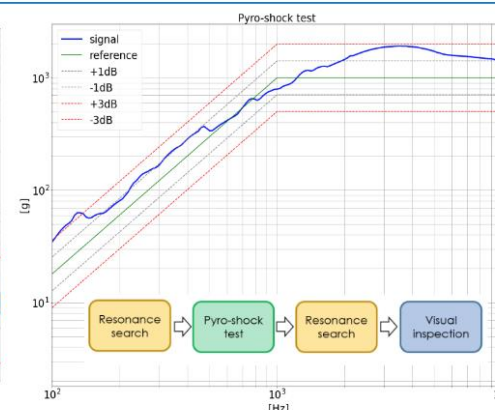
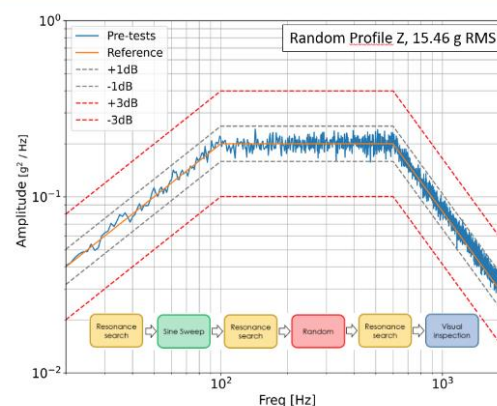


8 Strip- X detectors and 3 Strip-Y detectors built and tested

SMT Beam Tests

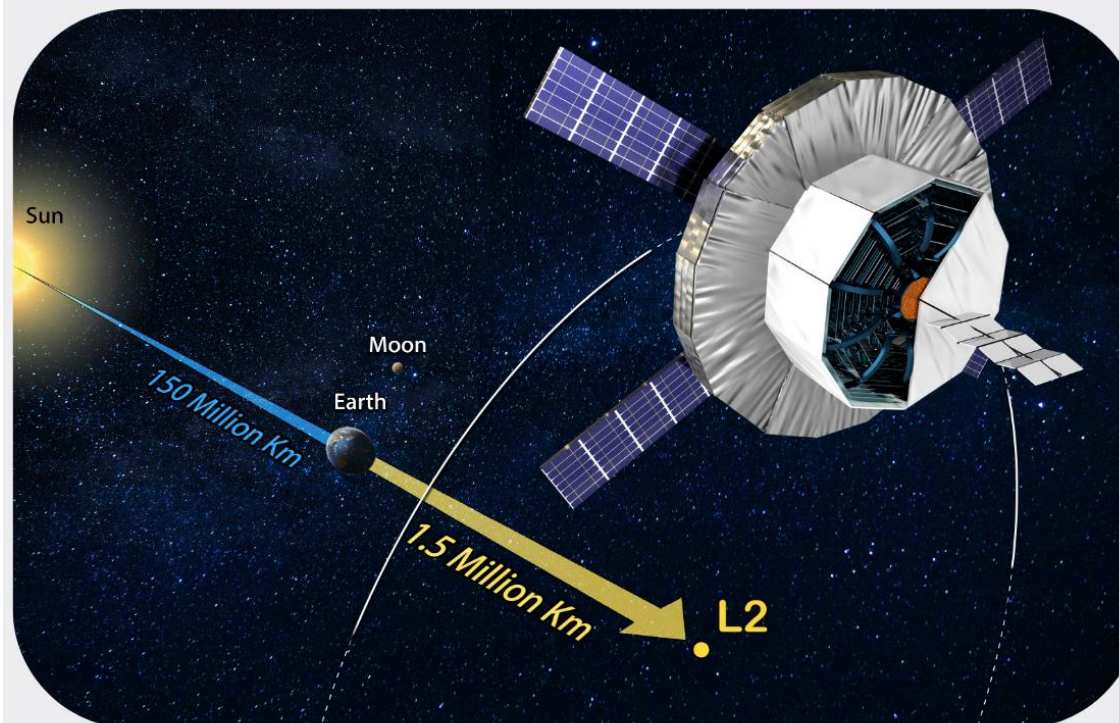


SMT single module Space Qualification - Mechanical Tests



Progressing in particle astrophysics with the Antimatter Large Acceptance Detector In Orbit

ALADInO



High Temperature Superconducting Magnetic Spectrometer in space

Acceptance $> 10 \text{ m}^2\text{sr}$
Antimatter measurements up to 20 TV
Established technologies for detection of
particles in space

5-year operations in L2

Payload Weight $< 6.5 \text{ t}$
Payload power consumption 3 kW
Compact volume (fits Ariane launcher)

Roadmap for mission opportunity

mid 2030s: ALADInO Pathfinder
mid 2040s: Operations in L2
by 2050: Unprecedented results

<https://doi.org/10.3390/instruments6020019>



Matteo Duranti



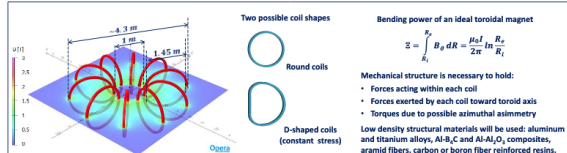
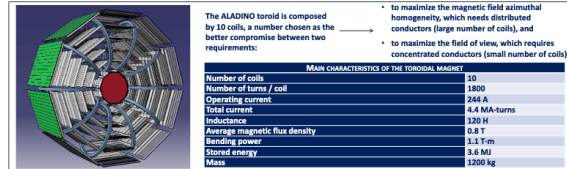
The Superconducting Space Magnet of the ALADiNO Spectrometer

Riccardo Musenich (INFN - Genova)
on behalf of the ALADiNO Collaboration



ALADiNO (Antimatter Large Acceptance Detector IN Orbit) is a large acceptance magnetic spectrometer based on a novel superconducting magnet technology, equipped with a silicon tracker and a 3D isotropic calorimeter. It is conceived to study anti-matter components of the cosmic radiation in an unexplored energy window which can shed light on new phenomena related to the origin and evolution of the Universe, as well as on the origin and propagation of cosmic rays in our galaxy. For more detailed information on the detector see poster presentation "ALADiNO: an Antimatter Large Acceptance Detector IN Orbit" by Matteo Duranti.

The generation of the magnetic field within ALADiNO is provided by a superconducting toroidal magnet. A toroidal magnet allows confining its field within the coils, leaving light stray field on other parts of the satellite. Moreover, it minimizes the dipole moment thus limiting the interaction with the environmental field (either geomagnetic or interplanetary) and consequently forces and torques on the spacecraft.



Superconducting space magnets - Main requirements:

- (i) low mass budget, i.e. high stored energy to mass ratio
- (ii) low power consumption, i.e. efficient cryogenics
- (iii) no liquid helium
- (iv) very high stability

low density materials - high current density

efficient cryocoolers and cryogenic heat pipes - low heat load

high temperature superconductors (REBCO or Magnesium Diboride)

High temperature superconductors (HTS) allows operating the magnet at temperature between 15 K (MgB₂) and 40 K (REBCO). High temperature leads to:

- more efficient cryogenics
- higher stability respect to quench triggering disturbances due to higher specific heat, therefore to higher enthalpy margin.

After a trade-off, it was chosen to use REBCO (Rare Earths Barium Copper Oxide). State of the art, 4 mm wide, 0.1 mm thick, REBCO tapes have critical current $I_c(3.7, 40 K) > 300 A$.

Further developments in conductor performances can lead to the reduction of the number of turns.

Despite quench of HTS magnets is unlikely, in case it happens, protection is known to be a major issue. Possible solution: no-insulation technique (actually, controlled insulation) which allows current diffusion and protects the coils.

The ALADiNO magnet is assumed to operate at $T \approx 40 K$, cooled by cryocoolers

Thermal radiation power coming from the several sources will be intercepted by a series of radiation shields. A passive multi-layer sunshield, umbrella-like, will be used to intercept the radiation heat flux from sun.

To minimize the heat load, the magnet is meant to operate in persistent mode. Two methods are possible to charge the magnet: a power supply with disconnectable current leads or a flux pump. The latter is an attractive solution which avoid moving parts and limit the power supply size.

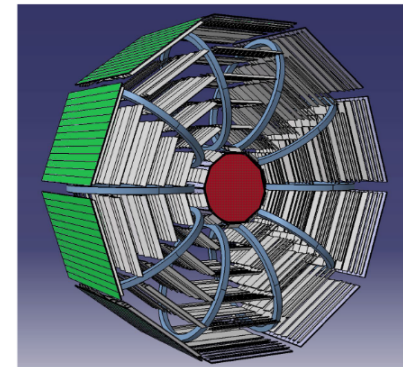
ALADiNO (Antimatter Large Acceptance Detector IN Orbit) is a large acceptance magnetic spectrometer based on a novel superconducting magnet technology, equipped with a silicon tracker and a 3D isotropic calorimeter. It is conceived to study anti-matter components of the cosmic radiation in an unexplored energy window which can shed light on new phenomena related to the origin and evolution of the Universe, as well as on the origin and propagation of cosmic rays in our galaxy. The generation of the magnetic field within ALADiNO is provided by a superconducting toroidal magnet. A toroidal magnet allows confining its field within the coils, leaving light stray field on other parts of the satellite. Moreover, it minimizes the dipole moment thus limiting the interaction with the environmental field (either geomagnetic or interplanetary) and consequently forces and torques on the spacecraft.

The coils will be wound with tapes based on High Temperature Superconductors (HTS), specifically REBCO (Rare Earths Barium Copper Oxide) tape. Such a conductor allows operating the magnet at temperature up to 40 K, thus avoiding liquid helium cryogenics and providing high stability with respect to quench-trigger disturbances. The latter is related to the specific heat capacity at 40 K of solid materials which is two order of magnitude higher respect to the values at 4.2 K, so that dramatically increases the enthalpy margin of the magnet.

The ALADiNO magnet is assumed to operate at $T \approx 40 K$, cooled by cryocoolers. To minimize the heat load, the magnet is meant to operate in persistent mode. Two methods are possible to charge the magnet: a power supply with disconnectable current leads or a flux pump. The latter is an attractive solution which avoid moving parts and limit the power supply size.

MAIN CHARACTERISTICS OF THE TOROIDAL MAGNET

Number of coils	10
Number of turns / coil	1800
Operating current	244 A
Total current	4.4 MA-turns
Inductance	120 H
Average magnetic flux density	0.8 T
Bending power	1.1 T-m
Stored energy	3.6 MJ
Mass	1200 kg



Other Astrophysics Detectors

Materials analysis

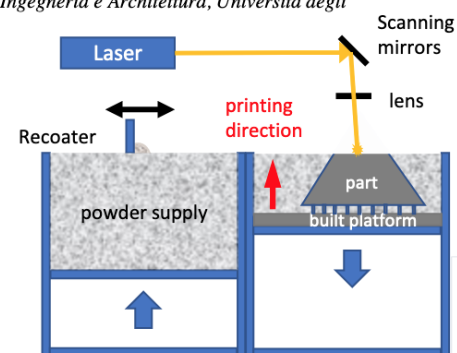


Study on properties of AISI 316L produced by Laser Powder Bed Fusion for high energy physics applications

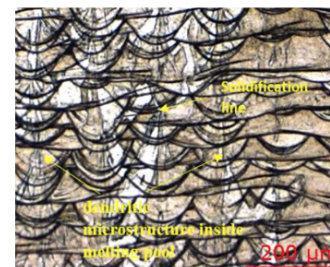
Cecilia Rossi^{1,*}, Francesco Buatier de Mongeot², Giulio Ferrando², Giacomo Manzato², Mickael Meyer³, Luigi Parodi¹, Stefano Sgobba³, Marco Sortino⁴, Emanuele Vaglio⁴

¹INFN Genoa, via Dodecaneso 33, 16146 Genoa, Italy; ²Dipartimento di Fisica, Università degli Studi di Genova, via Dodecaneso 33, 16146 Genoa, Italy; ³CERN, 1211 Geneva 23, Switzerland; ⁴Dipartimento Politecnico di Ingegneria e Architettura, Università degli Studi di Udine, via delle Scienze 206, 33100 Udine, Italy;

Nowadays additive manufacturing is catching on and spreading across various fields at an astonishing rate. High energy physics, where materials are often exposed to special environmental conditions, is also starting to use this technology. The aim of this paper is to compare traditional and 3D printed stainless steel AISI 316L products with an eye turned to the specific high energy applications. The manufactured samples are subjected to different heat treatments, including vacuum firing, which is usually adopted for ultra-vacuum applications. Experimental tests are carried out on a set of samples to analyse the material composition and to assess properties such as mechanical performance in cryogenic application, high radiation resistance and ultra-vacuum compatibility. Such analysis of the material behaviour allows weakness and strength of the technology to be identified, compared to traditional AISI 316L.



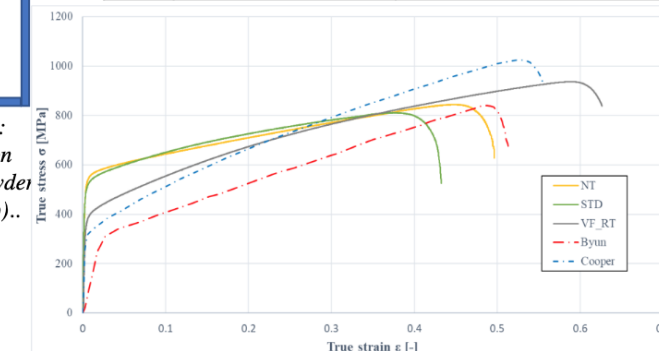
Selective laser melting working principle: recoater spreads a metallic powder bed on built platform, laser selectively melts powder part is build layer by layer (bottom to top)..



Different heat treatments:

- no difference in ferrite content
- no difference in the magnetic permeability

	Ferrite content check (Ferriscope FMP30)	Magnetic permeability (Magnetoscope 1.069)
NT	0.14±0.02 %	1.004 ± 0.004
STD	0.15±0.02 %	1.004 ± 0.004
VF	0.1±0.02 %	1.004 ± 0.004



Comparison of true stress strain curves at RT: AISI 316L AM parts subjected to different heat treatment vs. bulk parts.

NT (no heat treatment);
STD (standard h.t.): 180°C/h to 550°C; stable 6h; cool down;
VF (vacuum firing h.t.): 200°C/h to 950°C; stable 2h; cool down